HYDROGEN PRODUCTION FOR FUEL CELLS VIA REFORMING COAL-DERIVED METHANOL

41850R02.pdf

Quarterly Technical Progress Report
Reporting Period Start Date: January 1, 2004
Reporting Period End Date: March 31, 2004
Principal Author: Paul A. Erickson
Report Issue Date: April 2004
DOE Award Number: DE-FC26-03NT41850
Submitting Organization:

The Regents of the University of California, Davis
One Shields Avenue
Davis, California 95616

DISCLAIMER

This report was prepared as an account of work sponsored by an agency of the United States Government. Neither the United States Government nor any agency thereof, nor any of their employees, makes any warranty, express or implied, or assumes any legal liability or responsibility for the accuracy, completeness, or usefulness of any information, apparatus, product, or process disclosed, or represents that its use would not infringe privately owned rights. Reference herein to any specific commercial product, process, or service by trade name, trademark, manufacturer, or otherwise does not necessarily constitute or imply its endorsement, recommendation, or favoring by the United States Government or any agency thereof. The views and opinions of authors expressed herein do not necessarily state or reflect those of the United States Government or any agency thereof.

ABSTRACT

Hydrogen can be produced from many feed stocks including coal. The objectives of this project are to establish and prove a hydrogen production pathway from coal-derived methanol for fuel cell applications.

This progress report is the second report submitted to the DOE reporting on the status and progress made during the course of the project. This report covers the time period of January 1 – March 31, 2004. This quarter saw progress in five areas. These areas are:

1. Internal and external evaluations of coal based methanol and the fuel cell grade baseline fuel,
2. Experimental investigations of heat and mass transfer enhancement methods by flow field manipulation
3. Design and set up of the autothermal reactor,
4. Steam reformation of Coal Based Methanol as well as
5. Initial catalyst degradation studies

All of the projects are proceeding on or slightly ahead of schedule.

TABLE OF CONTENTS

EXECUTIVE SUMMARY

Hydrogen can be produced from many feed stocks including coal. The objectives of this project are to establish and prove a hydrogen production pathway from coal-derived methanol for fuel cell applications.

This progress report is the second report that will be submitted to the DOE reporting on the status and progress made during the course of the project. This report covers the time period of January 1 – March 31, 2004. This quarter saw progress in five areas. These areas are:

1. Internal and external evaluations of coal based methanol and the fuel cell grade baseline fuel,
2. Experimental investigations of heat and mass transfer enhancement methods by flow field manipulation
3. Design and set up of the autothermal reactor,
4. Steam reformation of Coal Based Methanol as well as
5. Initial catalyst degradation studies

All of the projects are proceeding on or slightly ahead of schedule. External and internal evaluations to compare the coal based methanol to the fuel cell grade methanol have been initiated. Preliminary results from both internal and external tests show that coal based methanol has significantly higher levels of petroleum hydrocarbons. Total chlorides, and sulfur were much higher than expected for both methanol samples that were evaluated externally. The sulfur and chloride tests are being validated. Tests of the fuels using an internal evaluation were also performed. Several differences between the coal-derived methanol and the baseline fuel cell grade methanol were described with one or more methods. GC-MS seems to be the best method for evaluating the methanols using the internal evaluation

Several pieces of equipment for the steam reformer (SR) and autothermal reformer (ATR) were purchased. ATR reactor design and set up continues and is expected to be operational in the next quarter. Additionally the ATR model developed has been valuable in sizing various components.

Data collection with baseline fuel (fuel cell grade) and with coal based methanol monitoring reactor performance was accomplished with the existing steam reformer set ups. The flow rate was varied to allow multiple space velocities and hysteresis of performance using coal-derived fuel was monitored. Preliminary studies present the large effect that flow fields can have on the hydrogen production process and add fundamental knowledge that will aid the construction and development of hydrogen production reactors. Further investigations into methods of enhancing the heat transfer characteristics were also performed.

Much progress has been made on the project funded by the Department of Energy during this reporting period. Substantial progress on the evaluation of the composition of coal-

derived methanol and the baseline fuel cell grade methanol has been made. Autothermal reactor design and construction has been initiated and continues with several integral pieces of equipment purchased and/or manufactured. Projects which have proven that coal derived hydrogen can be produced through steam reformation have been successful. Enhancement of heat transfer by bluff bodies has been proven for fuel cell grade methanol. Catalyst degradation projects have been started and analysis of reactor performance as well as catalyst analysis has taken place. Several projects are scheduled for the next quarter including validation of external evaluations of sulfur and chloride concentrations, further ATR reactor design and construction, continued preliminary evaluation of coal-based methanol in the steam reformers, and validation of heat transfer enhancement methods by use of bluff bodies.

EXPERIMENTAL

The following section describes the experimental methods used and developed during the reporting period for the following areas: external and internal evaluations of methanol, autothermal reactor design and construction, coal-derived methanol and water solution calibration, and steam reforming enhancement methods.

Evaluations of Methanol - External

Severn Trent Laboratories – Mobile (STL-Mobile) was selected to perform the external blind analysis to compare the coal-derived methanol to the fuel cell grade methanol. The analysis covered the amounts of methanol, ethanol, water, "mineral oil" as petroleum hydrocarbons, total chlorides, and total sulfur. The results from the external analysis are presented in the Results and Discussion section.

Evaluations of Methanol - Internal

Several different techniques were used to analyze the coal-derived methanol and the fuel cell grade methanol. The techniques are introduced below and the results are presented in the Results and Discussion section.

Nuclear Magnetic Resonance (NMR) spectroscopy Test

1ml samples of coal derived methanol and fuel cell grade methanol were added to ALDRICH NMR Tubes, 5mm Series 300, 7in length with 10ml deuterated water (D2O). Bruker DRX 500 operates at 11.746 Tesla or 500 MHz. Temperature range is from -150 to 180°C and stability is ± 0.2°C .Under strong magnetic field, structure of compounds and dynamic information with regard to injected samples can be achieved by means of analysis of signal acquired by injected electromagnetic wave at microsecond.

Liquid Chromatography-Mass Spectrometer (LC-MS) Test

The samples of coal derived methanol and fuel cell grade methanol were injected into a 150mM X 2.3 mM C18 column running 0.1% formic acid and acetonitrile at 200 micro liters /minute. Both UV (220nM) and mass spectral data were acquired on a ThermoFinnigan LCQ running in the positive mode. To begin with, spectrogray methanol for setting on the basis standard was used for comparing with fuel cell grade methanol and coal-derived methanol. However, mass spectrometry of spectrogray methanol did not show apparent results because spectroscopy methanol is less pure than both coal-derived methanol and fuel cell grade methanol.

Gas Chromatography-Mass spectrometer (GC-MS)

The samples of coal derived methanol and fuel cell grade methanol were injected into a DB-5MS column which have 0.32mm I.D., 30 meters length, and 0.25µm film thickness manufactured by Agilent Technology running Helium as carrier gas at 1 milliliters /minute. Mass spectral data was acquired on a Finnigan MAT ITS40. For each run, a

1ml sample was injected into Gas chromatograph manufactured by Varian. GC-MS test was carried on 5 times to get rid of column bleed and increase the accuracy. Mass range was from 50 to 550 amu and acquiring time was 17minutes. Initial column temperature was 75˚C and final column temperature increased up to 260˚C.

ATR Reactor Design and Construction

A model for autothermal reforming has been developed in LabVIEW and is currently undergoing changes to make it more efficient and user friendly. The model will be adapted to run on inputs of premix flowrate or multiple fuel inputs (water and methanol separately). Using this model, the final design of the autothermal reformer is complete and Parts & Identification drawings have been completed along with system schematic drawings, shown below in .

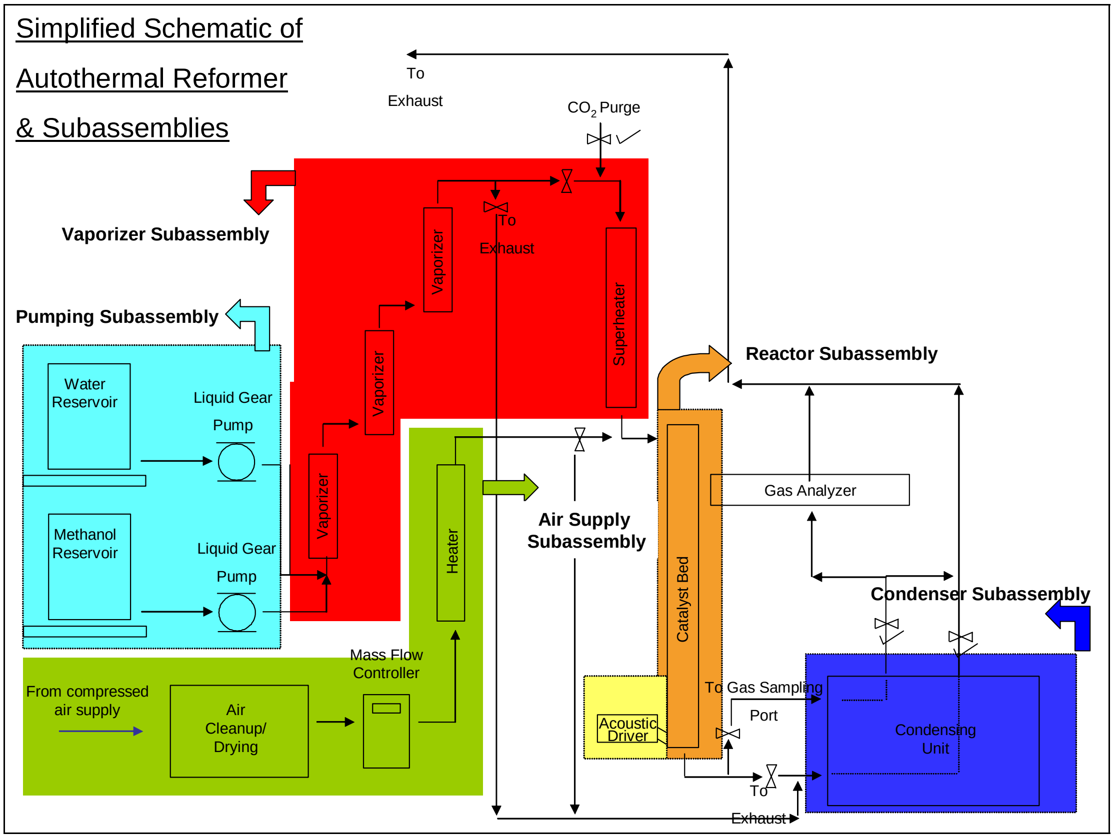

Figure 1: Simplified ATR schematic.

Machining on the catalyst bed housing has been completed and a work order has been issued for the welding the housing and its instrument ports. The catalyst housing is a 1.5" Sch 40 pipe of 12" length. The 12 thermocouple ports are placed in two rows of 6 on opposite sides of the reactor at a spacing of 2". There is a ¼" NPT fitting on the front of the housing that will adapt to a dynamic pressure transducer. Five 400W mineral insulated, nozzle band heaters wrap around the catalyst housing to supply any necessary heat.

For the air supply subsystem an Omega 1900-series mass flow controller (MFC) of 0-1 SLPM flowrate capacity has been tested and is operational. The LabVIEW control program for the MFC is under development. A second MFC will be ordered to allow testing at higher flowrates. The air clean up and drying unit has been delivered and work is being completed to incorporate it into the existing compressed air infrastructure in the laboratory. The air heating system has been ordered and received. It is a duplicate of one of the stages of the three stage vaporizer subsystem, utilizing a 400W cartridge heater.

One 0.020” K-type thermocouple and a package of 1/16” ceramic thermocouple insulators have been ordered so that testing of specially manufactured thermocouple probes can be tested before multiple units are ordered. All other necessary equipment has been ordered including pressure gauges, pressure transducers, and Swagelok compression fittings, adapters, and unions. The catalyst was tested with wrapping material and it was confirmed that it fits snuggly inside the 1.65” ID catalyst housing.

A draft of a paper being written for the ASME conference, International Mechanical Engineering Conference and R&D Expo, titled “Preliminary Modeling and Design of an Autothermal Reformer” is being finished and will submitted on April 30th.

Coal-derived Methanol and Water Solution Calibration

Due to the differences between the coal-derived methanol and the fuel cell grade methanol, a new calibration curve to determine the proper density for the coal-derived methanol/water premix for the steam reformer was developed.   represents the change of premix density at 24°C associated with different mass fractions of a coal-derived methanol/water solution. The purpose of this calibration is to calculate the conversion of coal-derived methanol. It is based on the assumption that only methanol and water can be condensed in the products. Other by-products may bias conversion ratio . In addition, the amount of condensate generated is dependent on sampling time, space velocity and overall temperature as well. To neglect error of conversion data, a minimum of 35-40 g of condensate liquid should be collected[2]. In addition, all condensate temperatures should be maintained at 0°C regardless of sampling time and space velocity. Moreover, before the condensate trap is opened, gas volume fraction indicated by gas analyzer (NOVA 7904 CM) should be identical with values associated with air. The Anton Parr handheld density meter was used for measuring density. It also has a thermocouple so that we can measure the density and corresponding temperature. After condensate trap is exposed, residual liquid droplets inside the trap is absorbed by a towel. Difference of weight before use towel was approximately 2 g from previous experiment. Even minute liquid droplets left inside the condensate trap should be absorbed to minimize the uncertainty of the conversion ratio. Then, mass fraction of unused coal-derived methanol and deionzied water can be calculated by means of density equation shown below

$$Y_{MeOH} = -5.5198\rho^2 + 4.5536\rho + 0.9422$$

Equation 1

Likewise, by means of mass fraction of both liquids, overall conversion can be calculated by the following mass basis equation.

$$Converion(\%) = \frac{m_{used \cdot MeOH} - m_{unused \cdot MeOH}}{m_{used \cdot MeOH}} \times 100$$

Equation 2

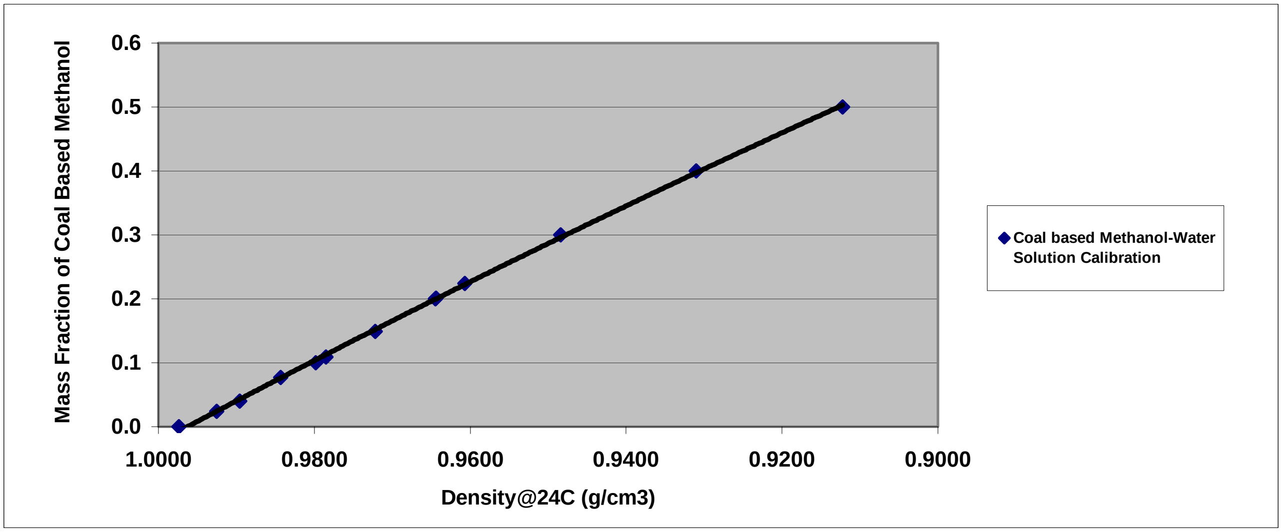

Figure 2: Coal-derived methanol/water solution calibration.

Steam Reformation Enhancement Methods

In a steam reforming process, heat transfers between reformate species and heat source can deeply affect the performance of the reaction. Changing the flow pattern and extending the residence time of the reformate inside the catalyst bed are expected to improve the heat transfer and decrease the temperature gradient inside the reactor. Placing bluff bodies inside the reformate pathways of the two steam-reforming reactors is expected to achieve this result. In this study, we designed one bluff body structure by composing of a disk and a ring to form a package. The material of the bluff body is made of 316 stainless steel metal plates, which is the same material as the reactor. Two sizes of bluff body structures were made to fit for two reactor dimensions. (For Reactor A, the disk diameter is 1/2 inch; I.D. of the ring is 1/2 inch, and its O.D. is 0.817 inch. For Reactor B, the disk diameter is 1.0 inch; ring: I.D. of the ring is 3/4 inch, and its O.D. is 1.368 inch.) The thickness of the two bluff body sizes are both 0.024 inch. Pictures of the two sizes of bluff body structures are shown in and . A schematic of bluff body inside the reactor B was shown in Figure 5.

Figure 3: Bluff body structures for Reactor A

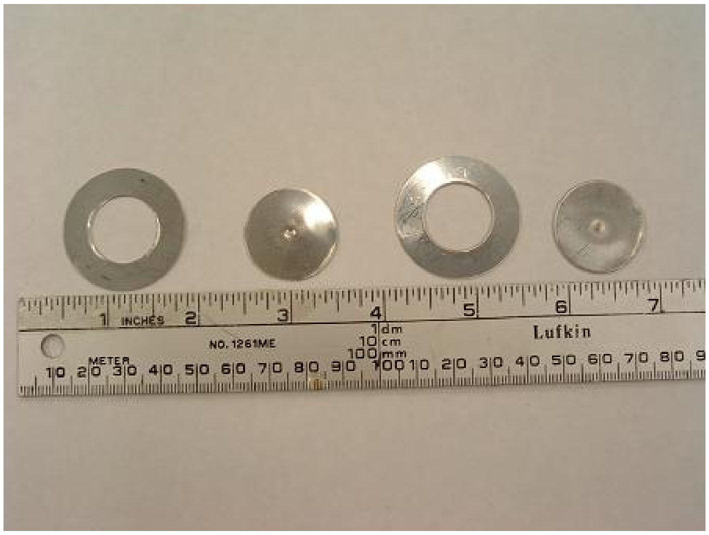

Figure 4: Bluff body structures for Reactor B

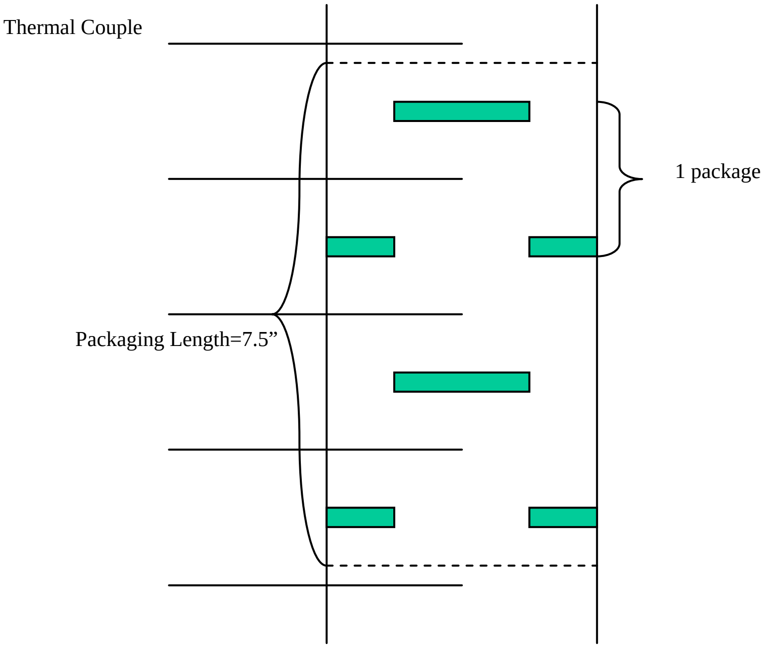

Error!

Figure 5: Cross section of bluff body arrangement inside Reactor B

The number of bluff body sets in reactor is expected to affect the reforming performance. In this study, package length density of the bluff body(defined as the number of bluff body sets divided by the length of the reactor) will be varied to investigate the effect of bluff bodies on a steam-reforming reactor.

RESULTS AND DISCUSSION

The following section presents results from the reporting period from the following areas: external and internal evaluations of methanol, preliminary results from the steam reformation of fuel cell grade and coal-derived methanol, hysteresis tests using coal-derived methanol, and steam reforming enhancements methods.

Evaluations of Methanol - External

The results from the first round of external testing of the coal-derived methanol and the fuel cell grade methanol are shown below in .

Table 1: External Analysis of both Coal-Derived Methanol and Fuel Cell Grade Methanol

	Coal-derived Methanol	Fuel cell grade Methanol
Ethanol(mg/l)	<8000	<8000
Methanol(mg/l)	740000	750000

Water (%)	0.02%	0.11%
Total Petroleum Hydrocarbon(mg/l)	17	5.9
Chloride(mg/kg)	16000	150
Sulfur(mg/kg) (ASTM-D-129-64)	112	298

Petroleum hydrocarbons, chlorides and sulfur compounds are all poison for fuel cell applications. In addition, higher hydrocarbons, chlorides and sulfur also lead to irreversible processes in both fuel cells and fuel processors. Both chloride and sulfur are lethal impurities because of chemical adsorption on the activate sites in the steam reformer. For example, after adsorption, mass diffusion problems may occur because of blocking the pores in the catalyst. Initial external testing reports that the coal-derived methanol has much more chloride than fuel cell grade methanol even though it should be maintained below 0.1ppm. Furthermore, sulfur should be also maintained below 1ppm even though both fuel cell grade methanol and coal-derived methanol greatly exceed that specification. A second round of external testing has been initiated to confirm the results of the initial testing.

Evaluations of Methanol – Internal

Nuclear Magnetic Resonance (NMR) spectroscopy Test

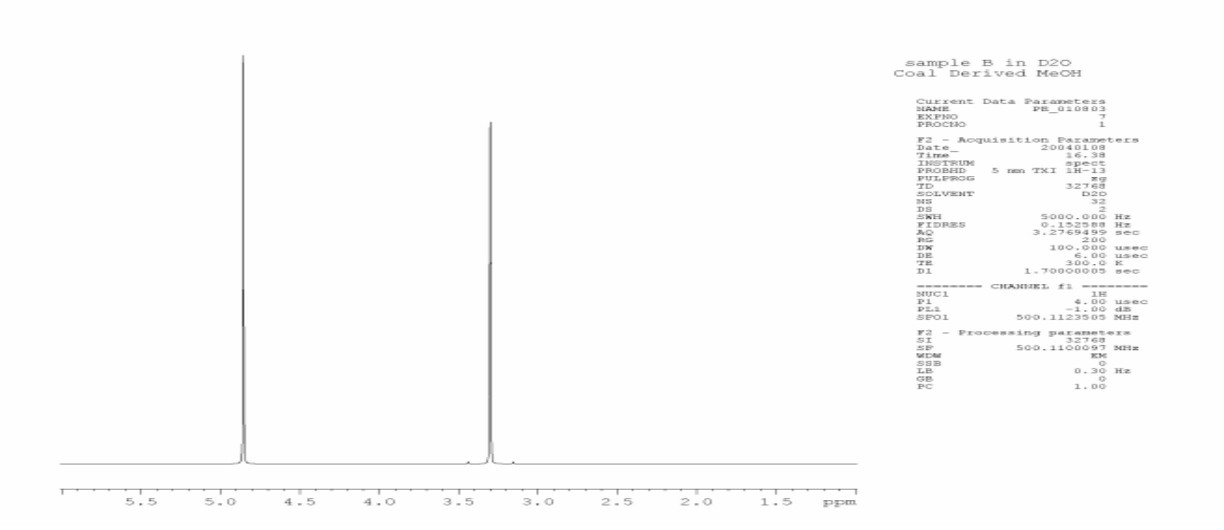

```
 sample B in D2O
Coal Derived MeOH

  Current Data Parameters
  NAME            PE_010803
  EXPNO                   7
  PROCNO                  1

  F2 - Acquisition Parameters
  Date_            20040108
  Time                16.38
  INSTRUM             spect
  PROBHD   5 mm TXI 1H-13
  PULPROG                zg
  TD                  32768
  SOLVENT               D2O
  NS                     32
  DS                      2
  SWH              5000.000 Hz
  FIDRES           0.152588 Hz
  AQ              3.2769499 sec
  RG                    200
  DW                100.000 usec
  DE                   6.00 usec
  TE                  300.0 K
  D1             1.70000005 sec

  ======== CHANNEL f1 ========
  NUC1                   1H
  P1                   4.00 usec
  PL1                 -1.00 dB
  SFO1          500.1123505 MHz

  F2 - Processing parameters
  SI                  32768
  SF            500.1100097 MHz
  WDW                    EM
  SSB                     0
  LB                   0.30 Hz
  GB                      0
  PC                   1.00
```

Figure 6: NMR spectrograph for Coal-Derived Methanol

ppm is methanol and another peak around 4.8 ppm is deuterated water solvent. NMR detection limit is relatively low compared with Liquid Chromatography/Mass Spectrometer (LC/MS) and Gas Chromatography/Mass Spectrometer (GC/MS).

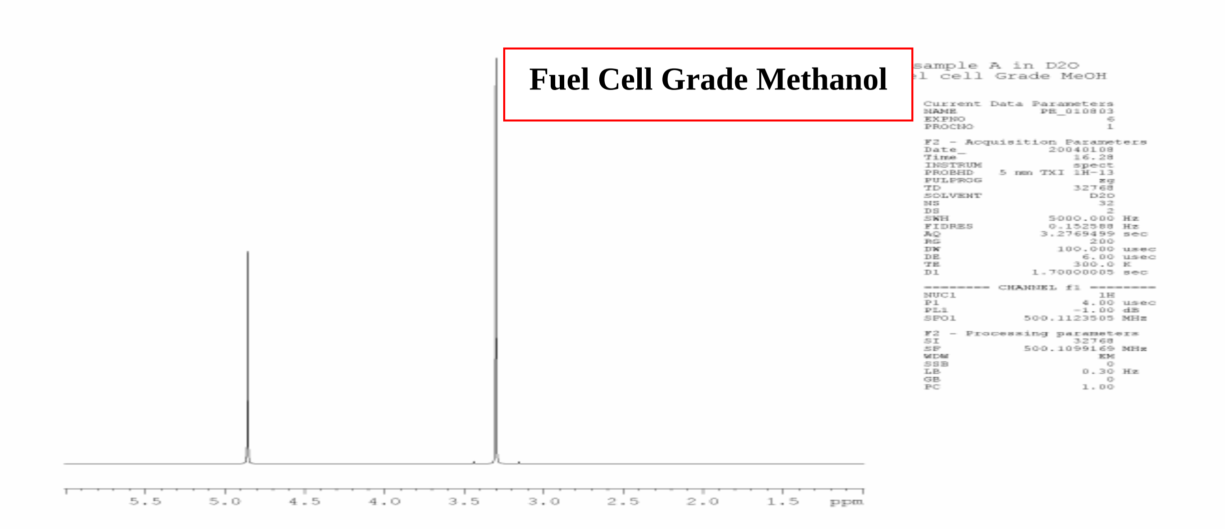

Figure 7: NMR spectrograph for Fuel Cell Grade Methanol

peak with coal-derived methanol. One peak from around 3.3ppm is methanol and another peak around 4.8ppm is deuterated water. Compared coal derived methanol to fuel cell grade methanol, there are no differences between coal-derived methanol and fuel cell grade methanol by means of NMR. Consequently, one of analysis method NMR is not sufficient for our methanol analysis because it couldn't detect low concentration impurities in both methanols. Even though there are methods to increase up to impurity concentrations to be allowable detection for NMR such as solid phase extraction and evaporation, those methods will be required in a large amount of methanol.

Liquid Chromatography-Mass Spectrometer (LC-MS) Test

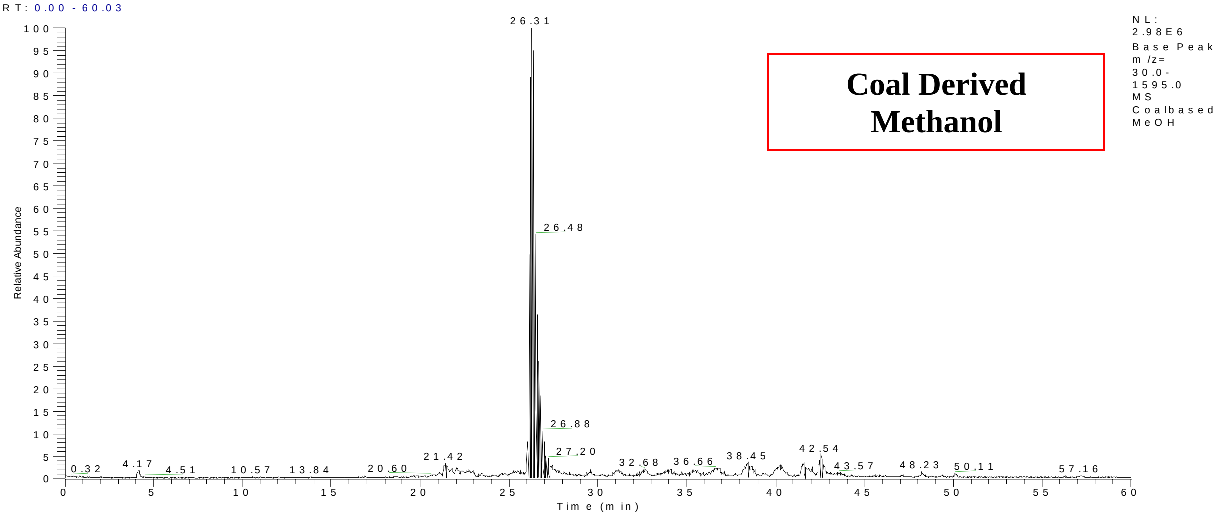

Figure 8: LC-MS time trace of Ionization for Coal-derived Methanol

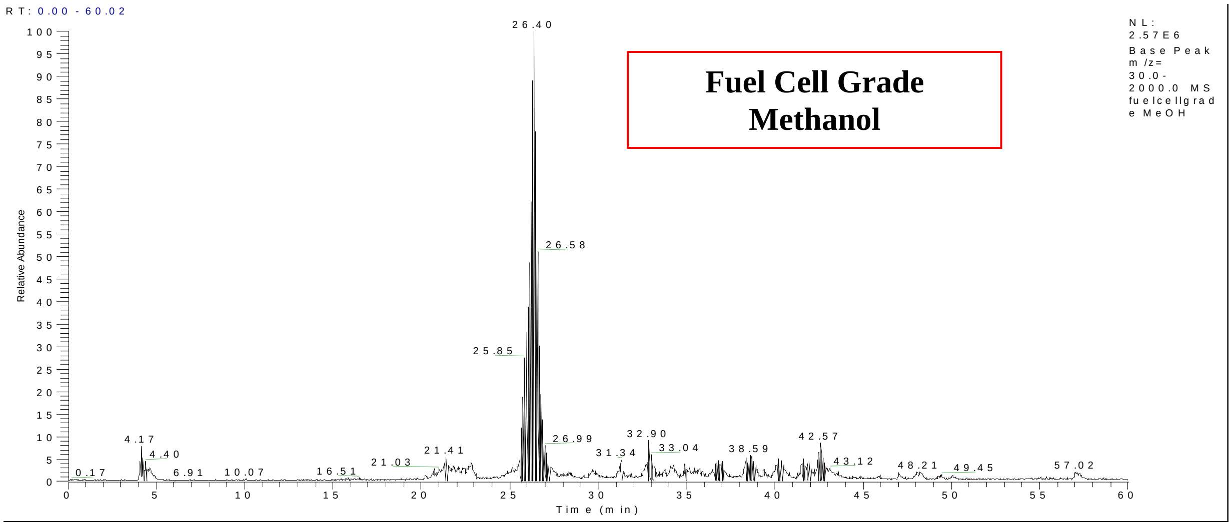

Figure 9: LC-MS time trace of Ionization for Fuel Cell Grade Methanol

Above those graphs, they represent ionized fraction compounds in methanol impurities. To begin with, C18 polar column was used which is usually applicable for huge molecular weight protein. Approximately, impurities molecular weights we found using LC-MS are over 500g/mol (i.e. higher hydrocarbon) responded by characteristic of column. However, only LC-MS can not be allowable to fully analyze impurity compounds so that elementary chemical analysis, Infrared (IR) Spectroscopy, increasing concentration and GC-MS might be needed.

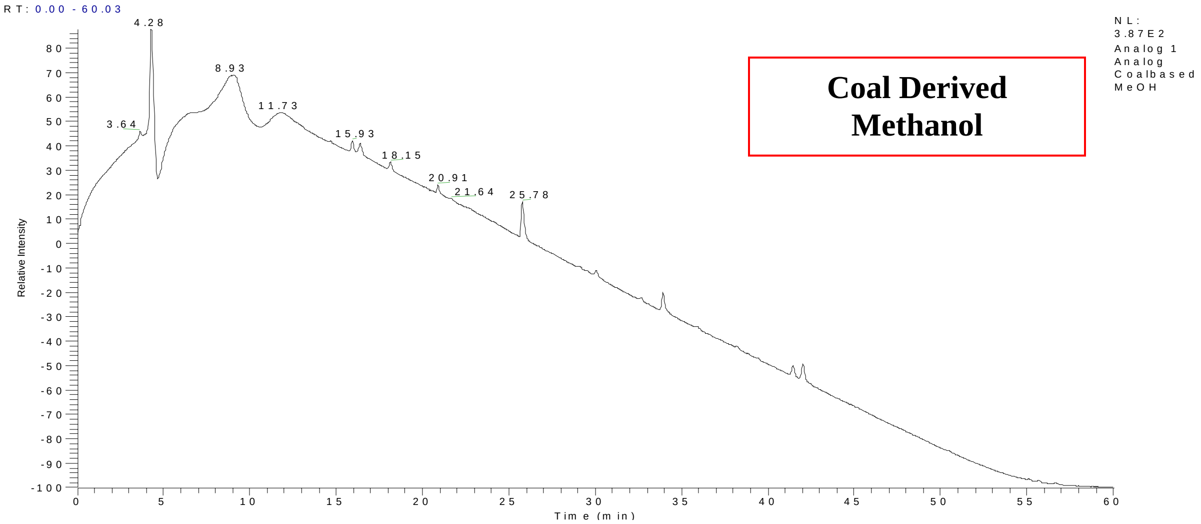

Figure 10: LC-MS time trace of UV detection for Coal-derived methanol

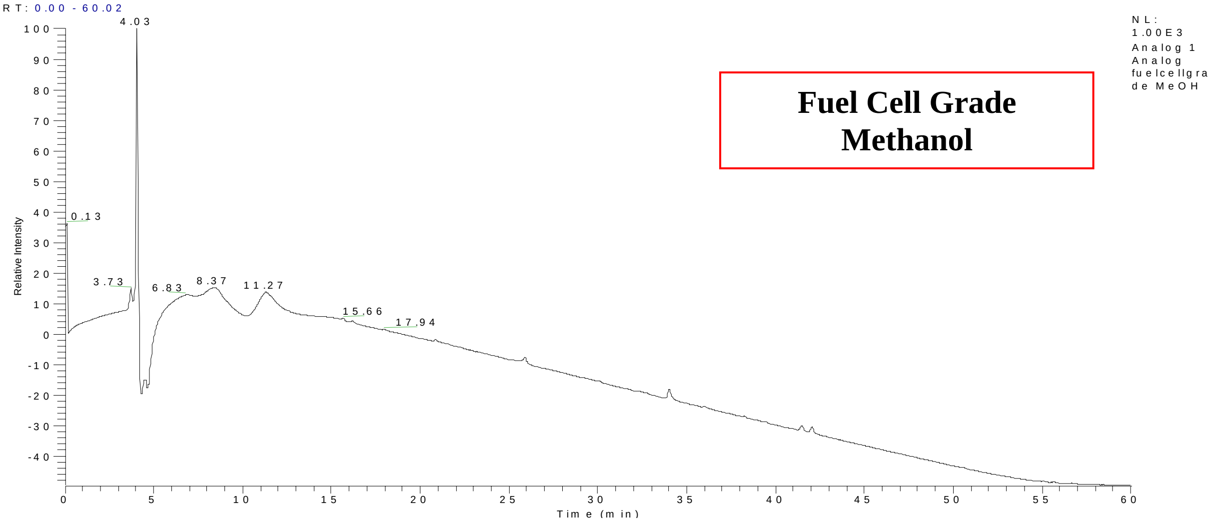

Figure 11: LC-MS time trace of UV detection for Fuel Cell Grade Methanol

Figure 10 and Figure 11 represents UV detection corresponded by both compounds and ionization over both coal derived methanol and fuel cell grade methanol.

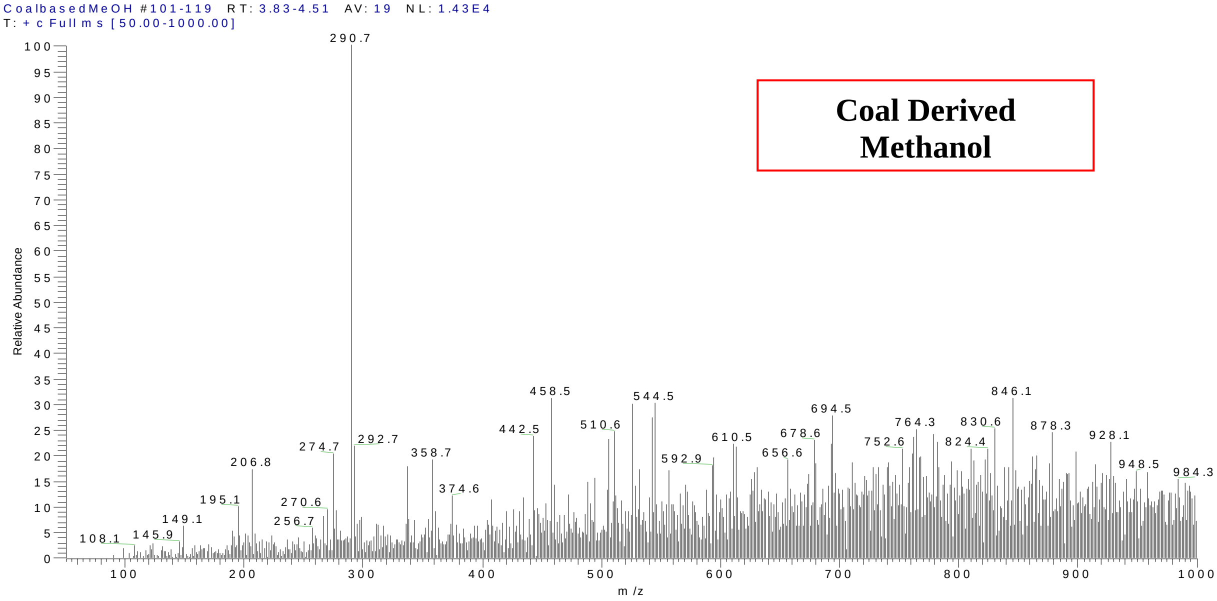

Figure 12: Mass spectrograph for Coal-derived from 3min83sec to 4min51sec

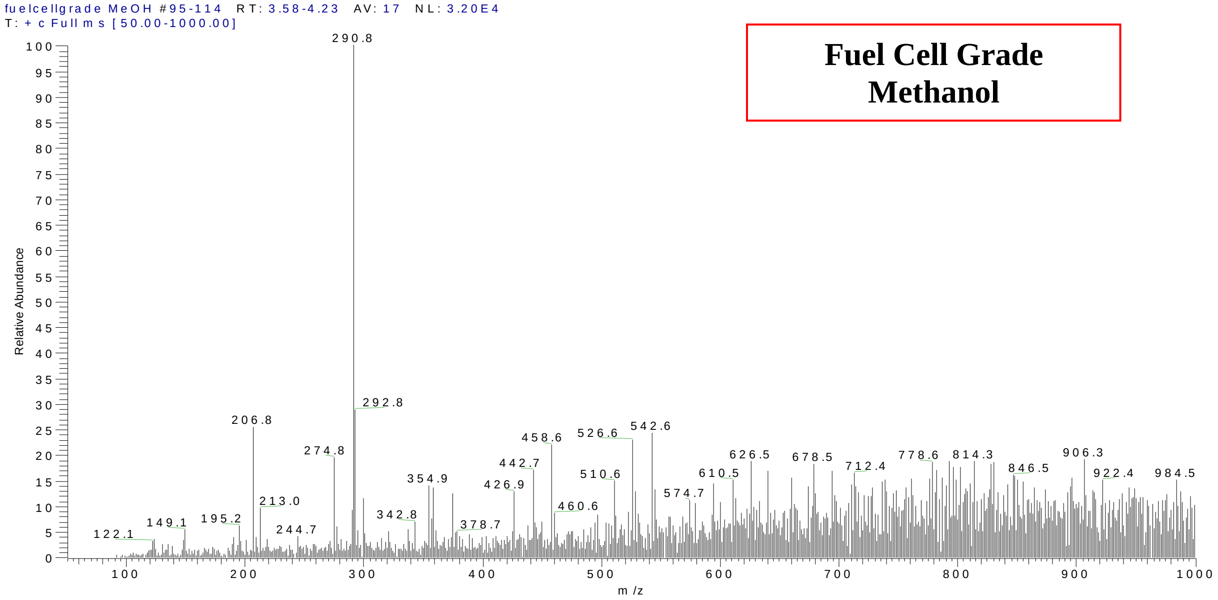

Figure 13: Mass Spectrograph for Fuel Cell Grade Methanol from 3min58sec to 4min24sec

In Figure 12 and Figure 13, two compounds have same base peak 290.8, mass fragment patterns and running time. It can be hardly evaluated with regard to molecular weight due to noise.

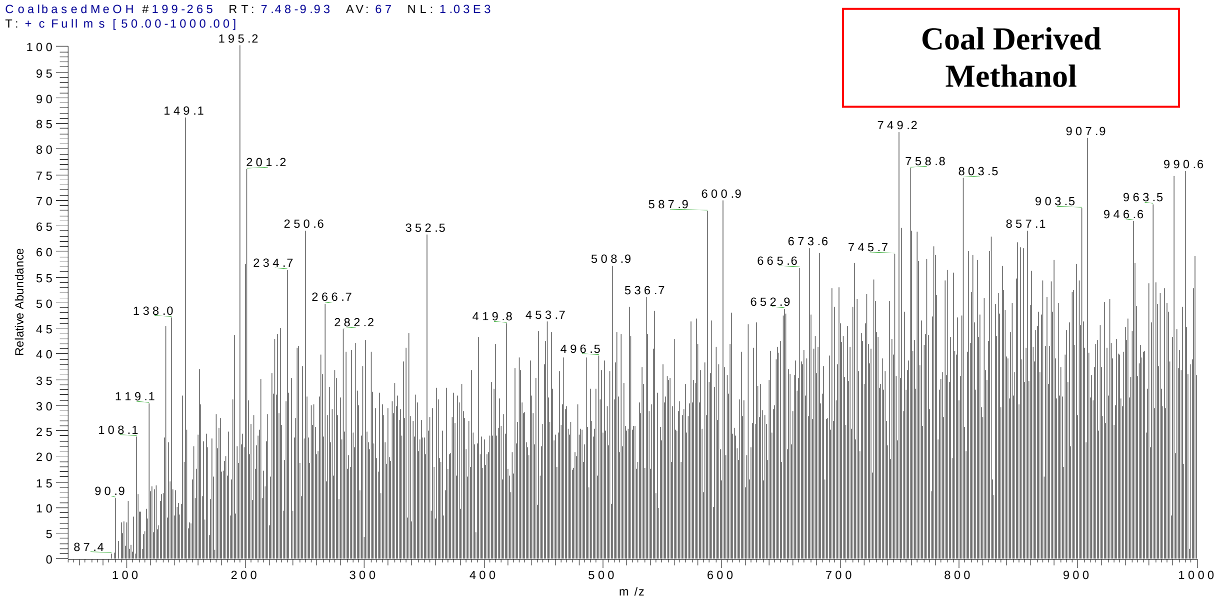

Figure 14: Mass Spectrograph for Coal-derived Methanol from 7min48sec to 9min93sec

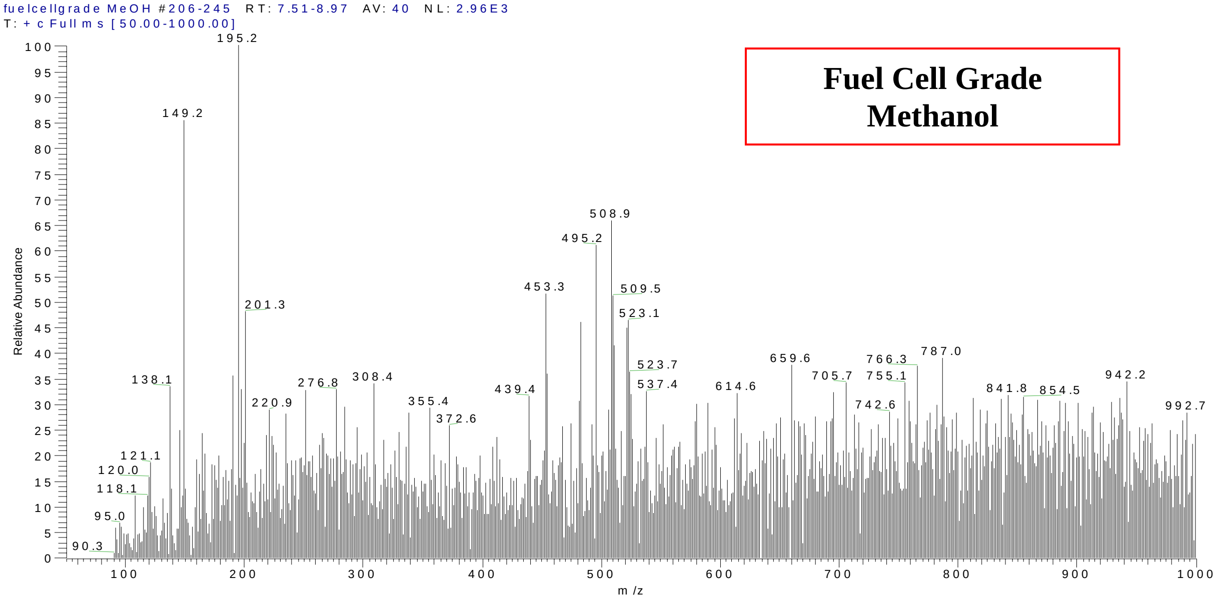

Figure 15: Mass Spectrograph for Fuel Cell Grade Methanol from 7min51sec to 8min97sec

In Figure 12 and Figure 13, two compounds have showed different mass fragment patterns regardless of a same base peak and running time. Figure 12 shows clear mass fraction patterns. However, Figure 13 is ambiguous and seems noisy.

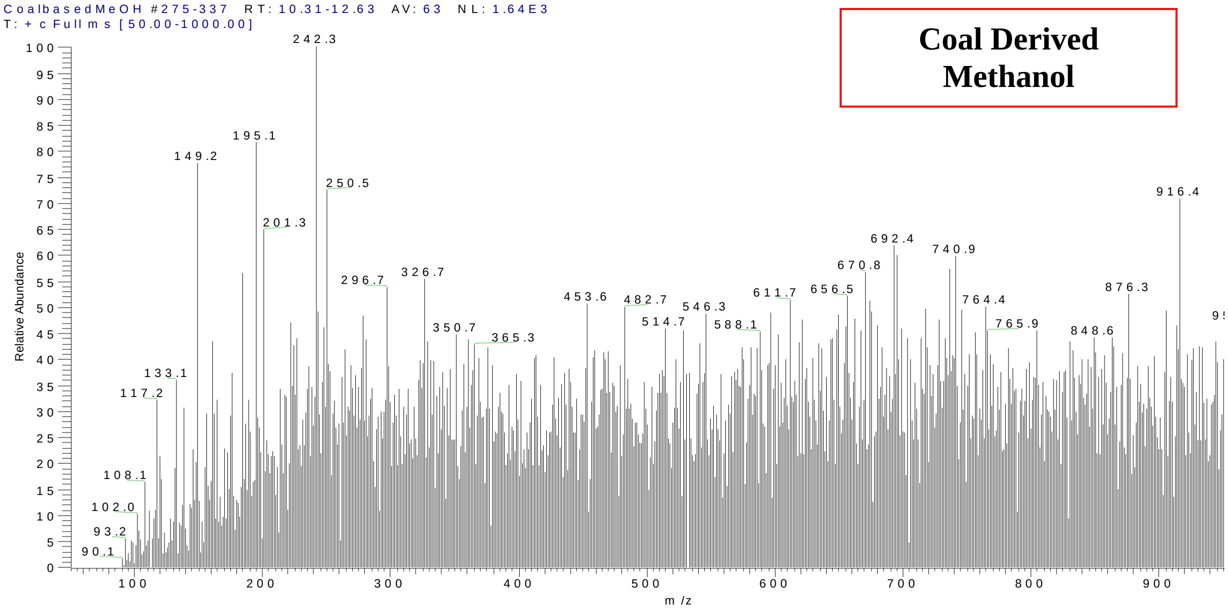

Figure 16: Mass Spectrograph for Coal-derived Methanol from 10min31sec to 12min63sec

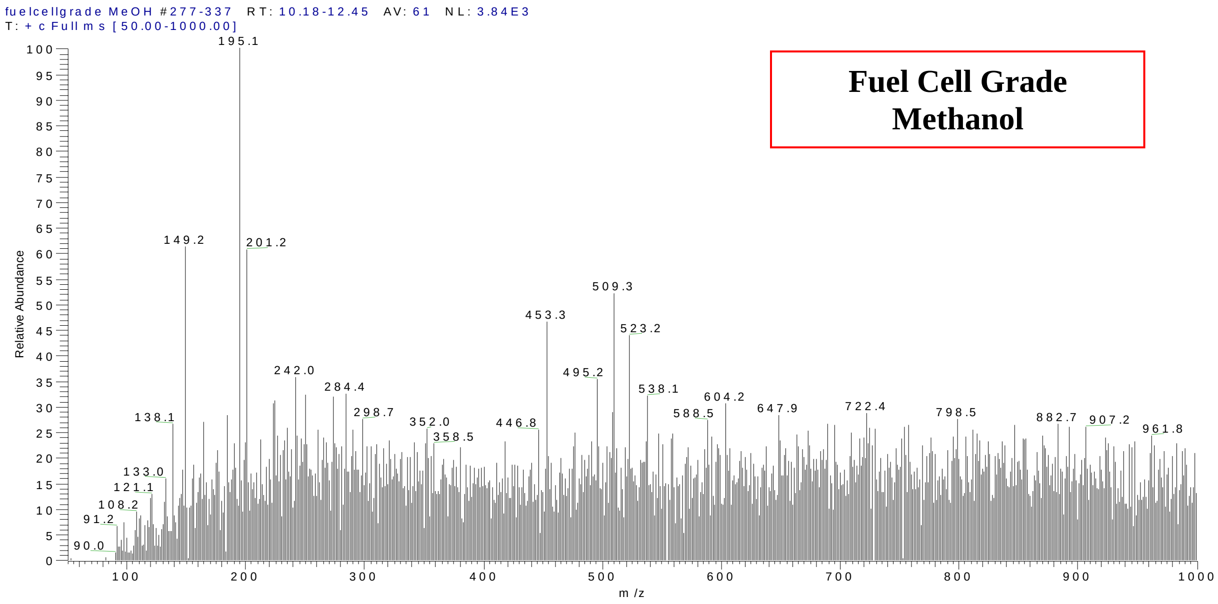

Figure 17: Mass Spectrograph for Fuel Cell Grade Methanol from 10min18sec to 12min45sec

In figure 16 and 17, two compounds show a different base peak and mass fraction pattern. Due to lots of noise, it can hardly be evaluated.

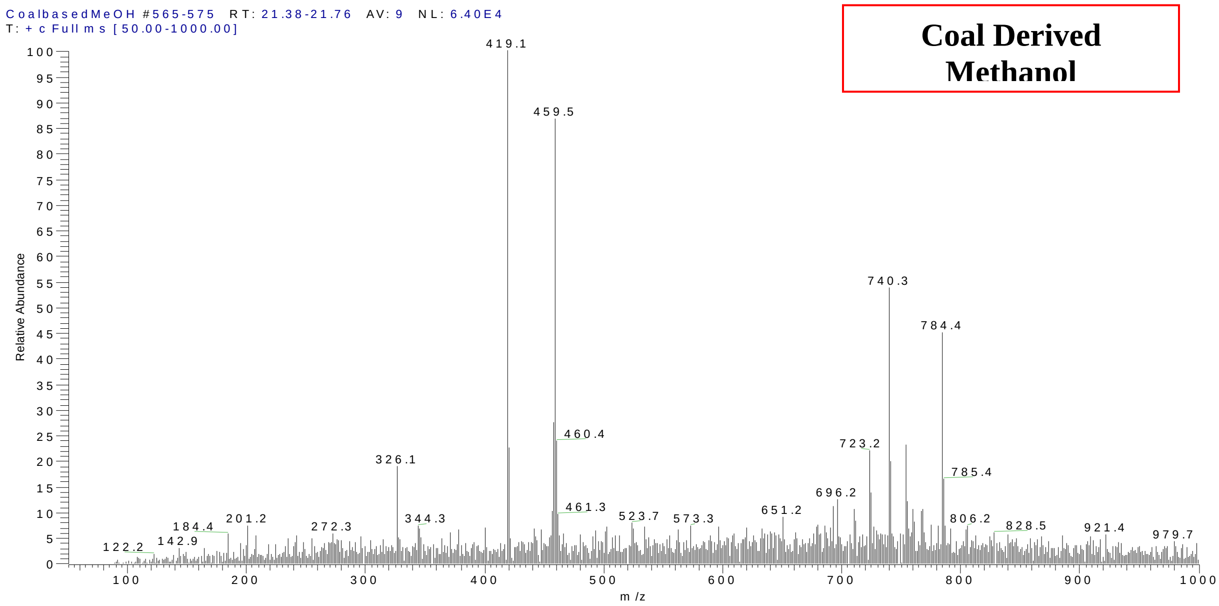

Figure 18: Mass Spectrograph for Coal-derived Methanol from 21min38sec to 21min76sec

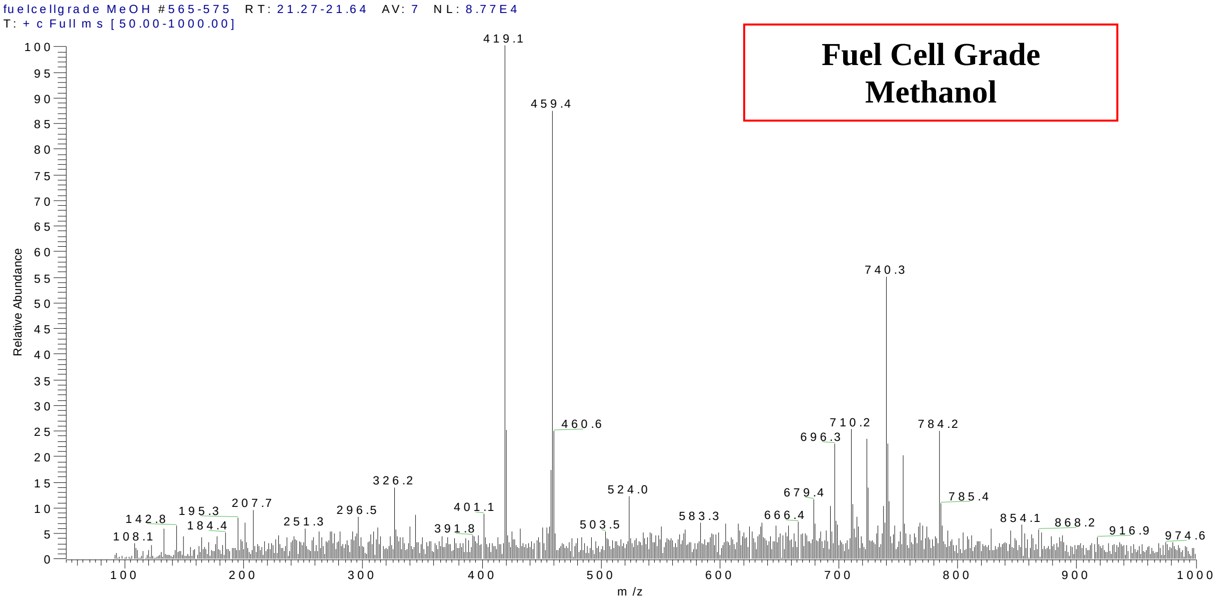

Figure 19: Mass Spectrograph for Fuel Cell Grade Methanol from 7min48sec to 9min93sec

In figure 18 and 19, two compounds have a same base peak 419.3, mass fragment patterns and running time. Those two higher hydrocarbon compounds which might have approximately 850~868 g/mol molecular weight are identical.

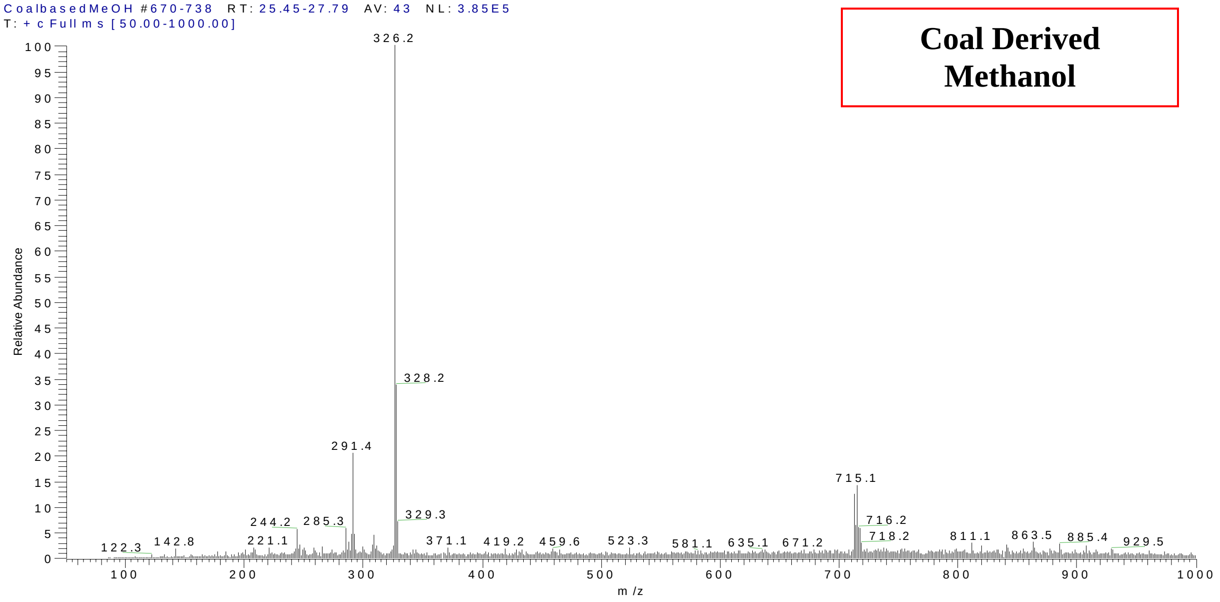

Figure 20: Mass Spectrograph for Coal-derived Methanol from 25min45sec to 27min79sec

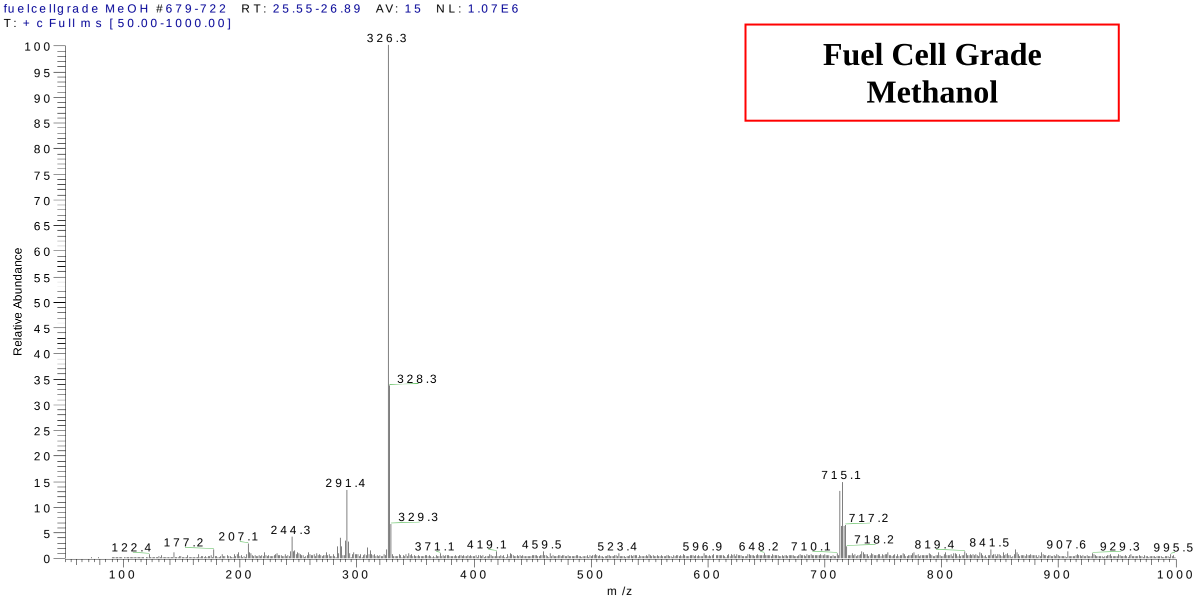

Figure 21: Mass Spectrograph for Fuel Cell Grade Methanol from 25min55sec to 26min89sec

In figure 20 and 21, two compounds are most abundant higher hydrocarbon compounds in both methanols. They have same mass fraction pattern and same base peak 326.3. Molecular weight might be approximately 819.4.

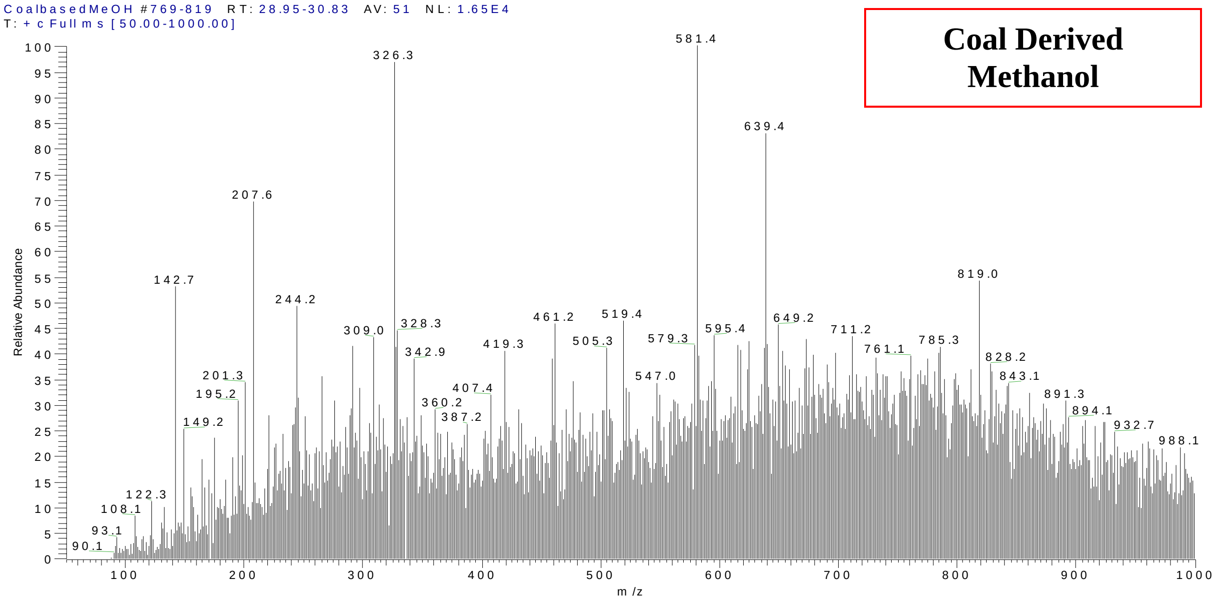

Figure 22: Mass Spectrograph for Coal-derived Methanol from 28min95sec to 30min83sec

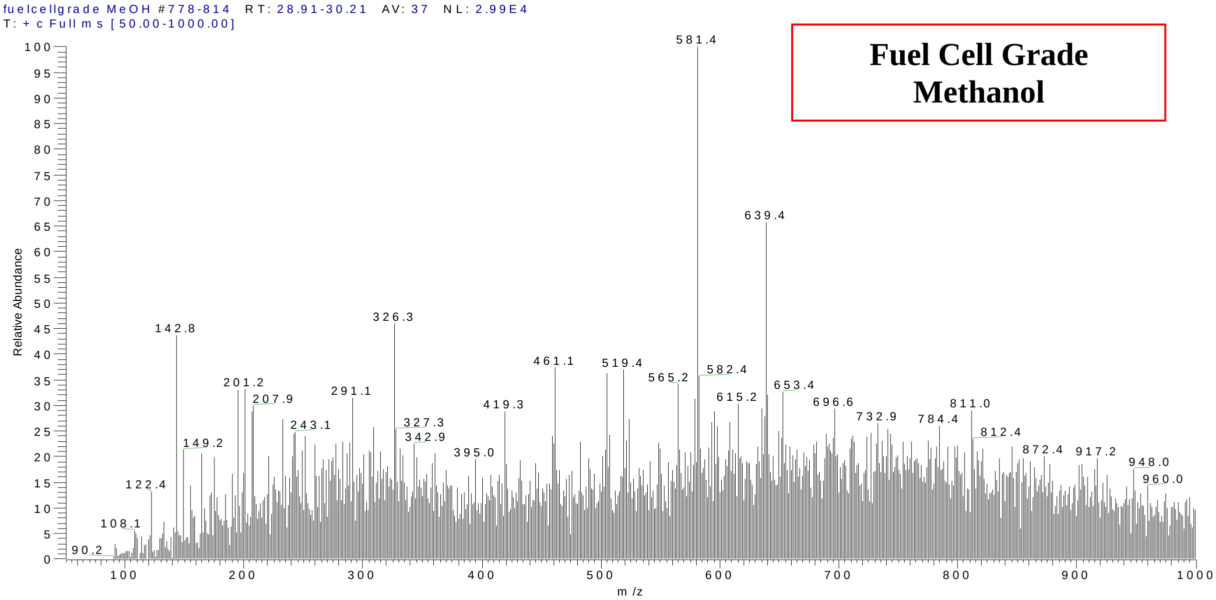

Figure 23: Mass Spectrograph for Fuel Cell Grade Methanol from 28min91sec to 30min21sec

patterns even though intensity of others mass fragment is different. It can be hardly evaluated with regard to molecular weight due to noise.

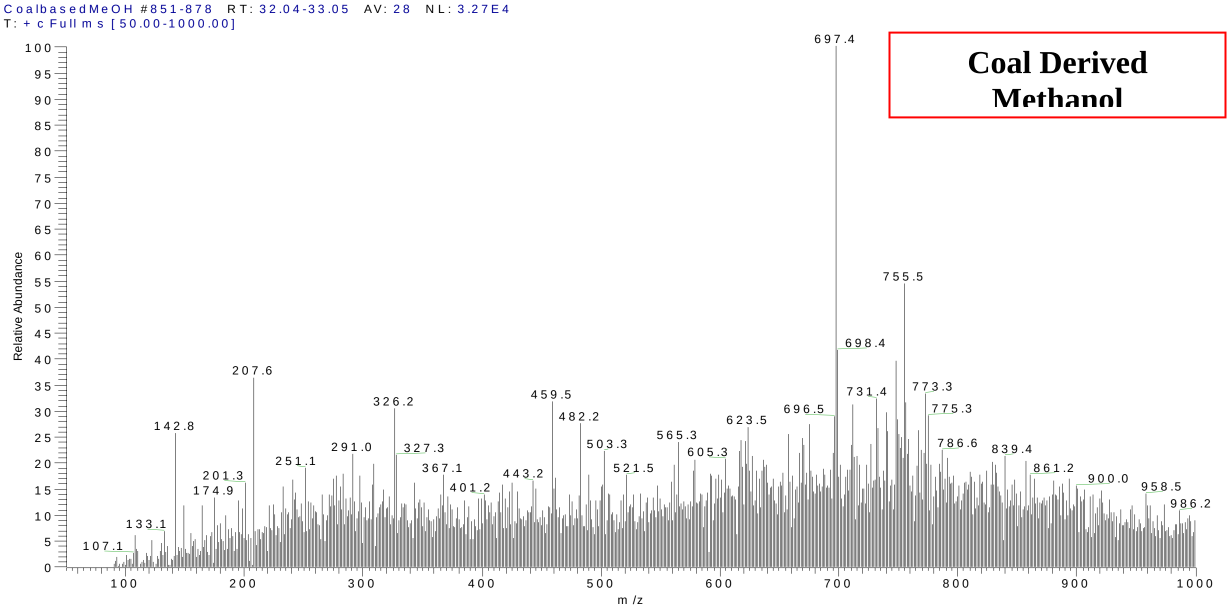

Figure 24: Mass Spectrograph for Coal-derived Methanol from 32min04sec to 33min05sec

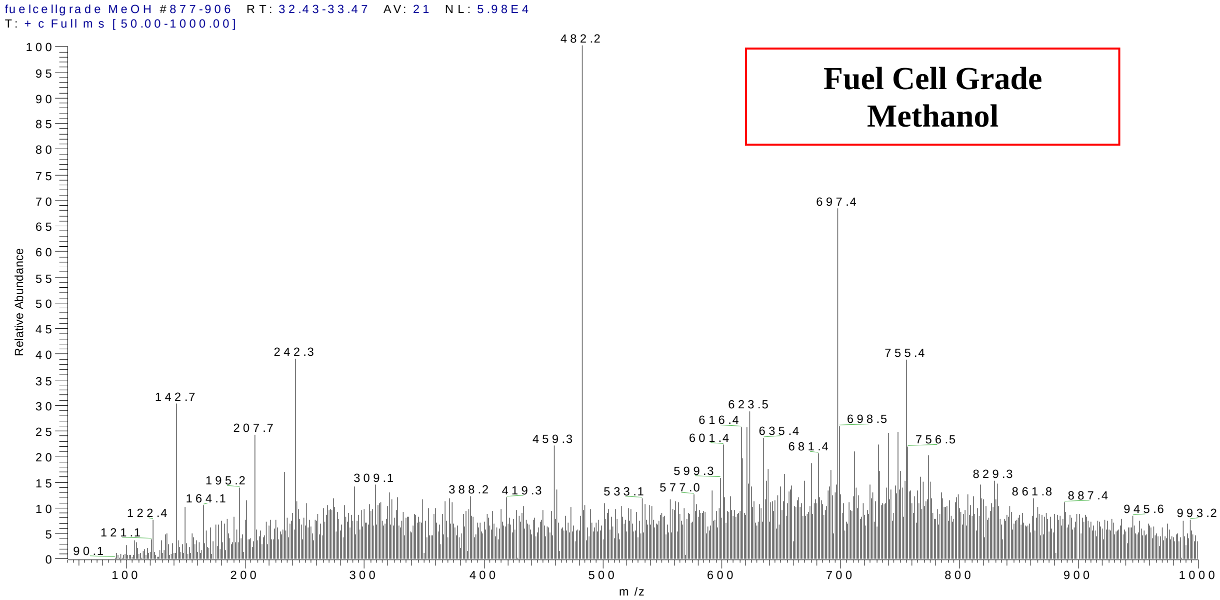

Figure 25: Mass Spectrograph for Fuel Cell Grade Methanol from 32min43sec to 33min47sec

Above two compounds are different because of different mass fragment patterns. In Figure 24 and 25, those graphs show different base peaks that one is 697.4 and another is 482.2. Both compounds are higher hydrocarbons which are over 800 g/mol molecular weight.

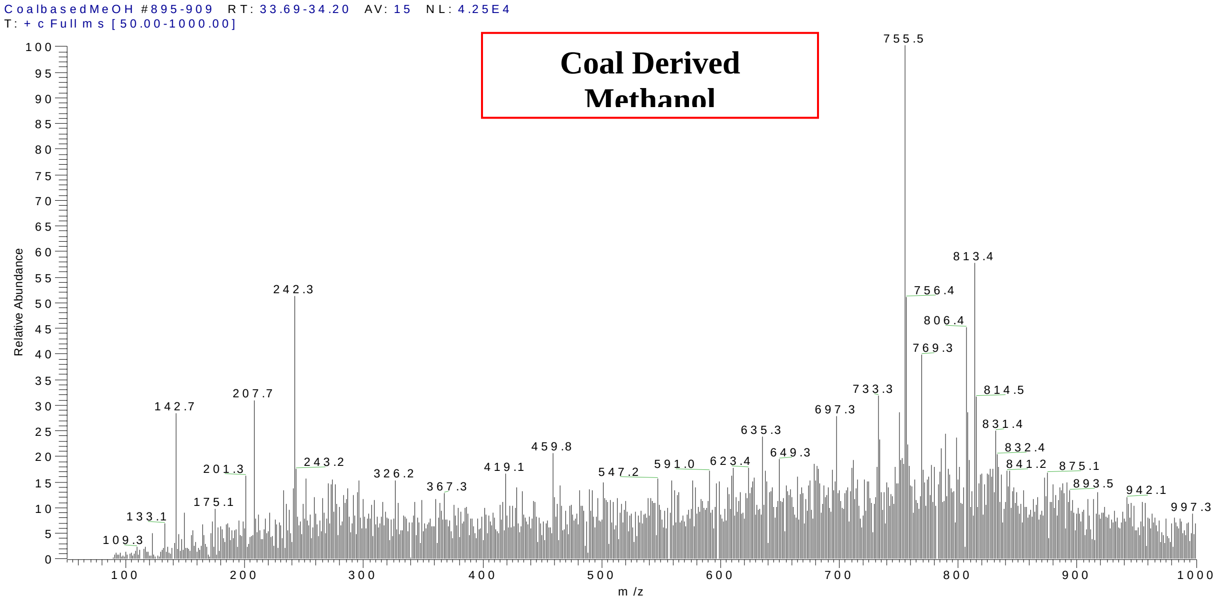

Figure 26: Mass Spectrograph for Coal-derived Methanol from 33min69sec to 34min20sec

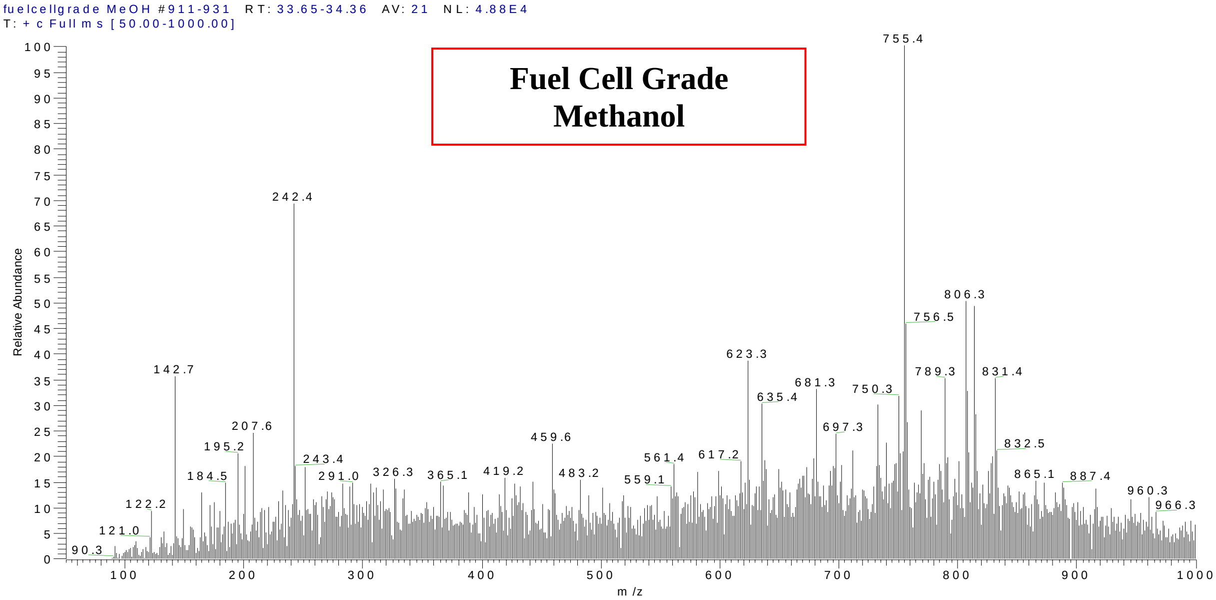

Figure 27: Mass Spectrograph for Fuel Cell Grade Methanol from 33min65sec to 34min36sec

In figure 26 and 27, those two compounds have same base peak 755.4. Coal-derived methanol has certain amounts of 813.5 and 814.5 mass fragment. However, it seems that there are not those mass fragments in fuel cell grade methanol. Obviously, those are higher hydrocarbons over 800 g/mol molecular weight.

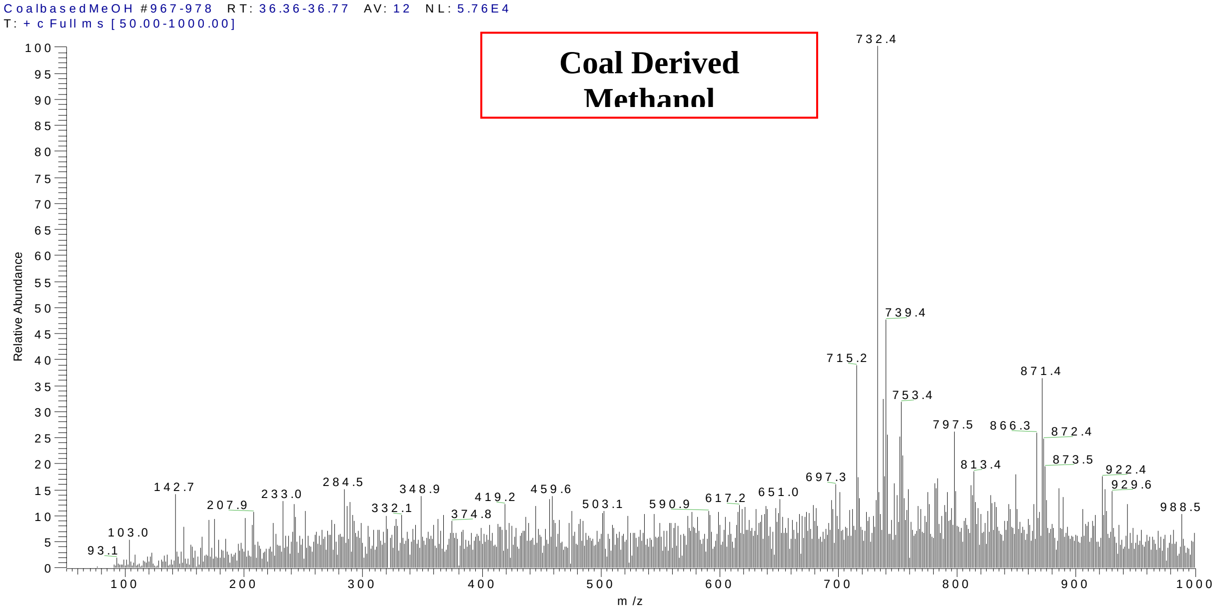

Figure 28: Mass Spectrograph for Coal-derived Methanol from 36min36sec to 36min77sec

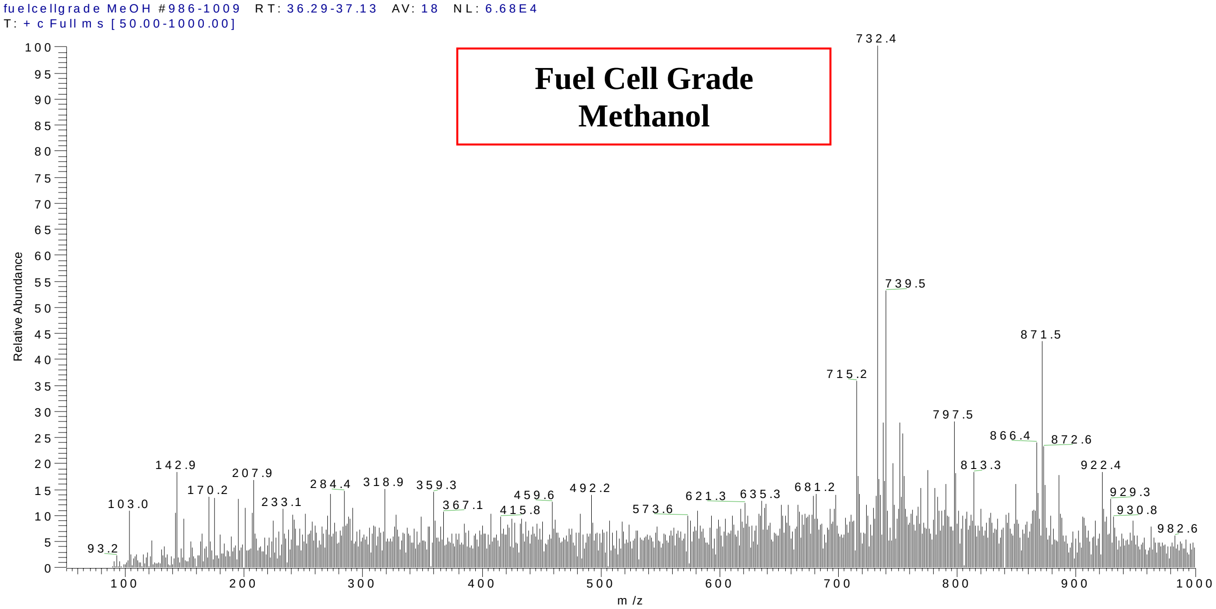

Figure 29: Mass Spectrograph for Fuel Cell Grade Methanol from 36min29sec to 37min13sec

In figure 28 and 29, two compounds have same base peak 732.4, mass fragment patterns, and same running time. Two higher hydrocarbon compounds which might have approximately over 900 g/mol molecular weight are identical

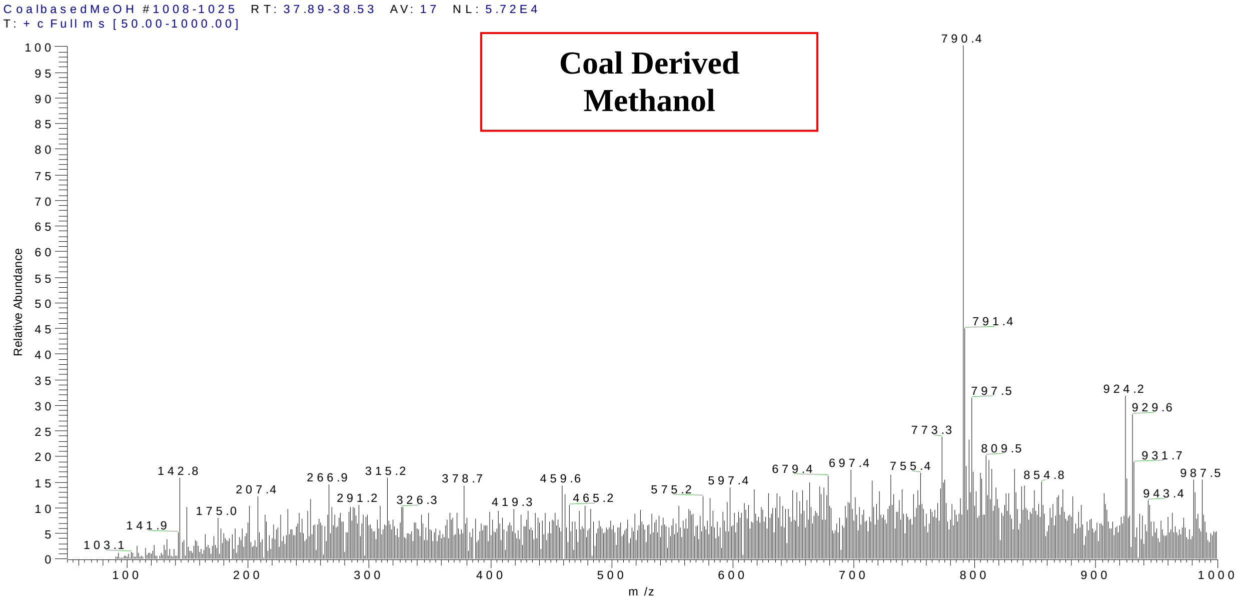

Figure 30: Mass Spectrograph for Coal-derived Methanol from 37min89sec to 38min53sec

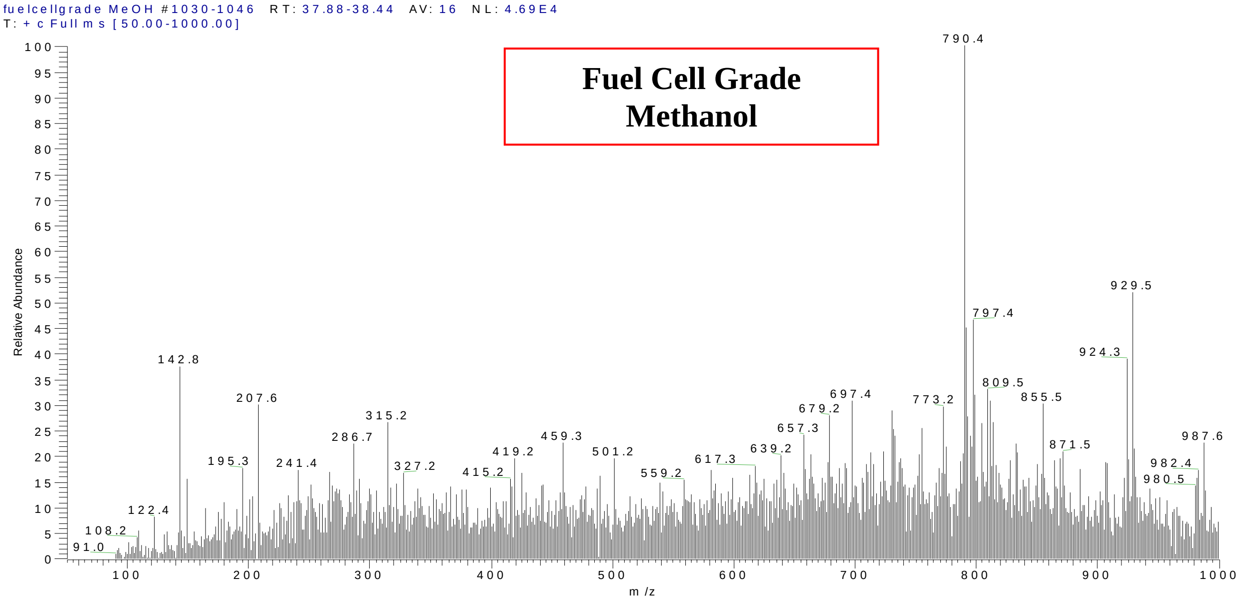

Figure 31: Mass Spectrograph for Fuel Cell Grade Methanol from 37min88sec to 38min44sec

In figure 30 and 31, two compounds have same base peak 790.4 and mass fragment patterns and running time. It can be hardly said that two compounds are identical regardless of same base peak, mass fragment and running time because of different intensity of mass fragment after base peak. Molecular weight of two compounds is over 980 g/mol.

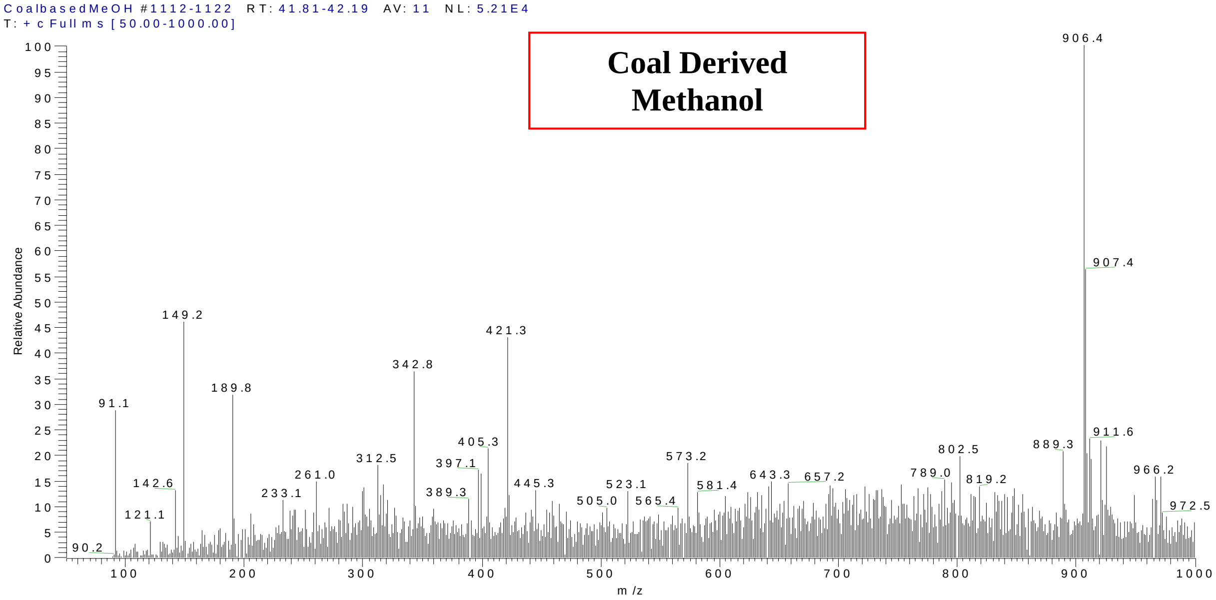

Figure 32:Mass Spectrograph for Coal-derived Methanol from 41min81sec to 42min19sec

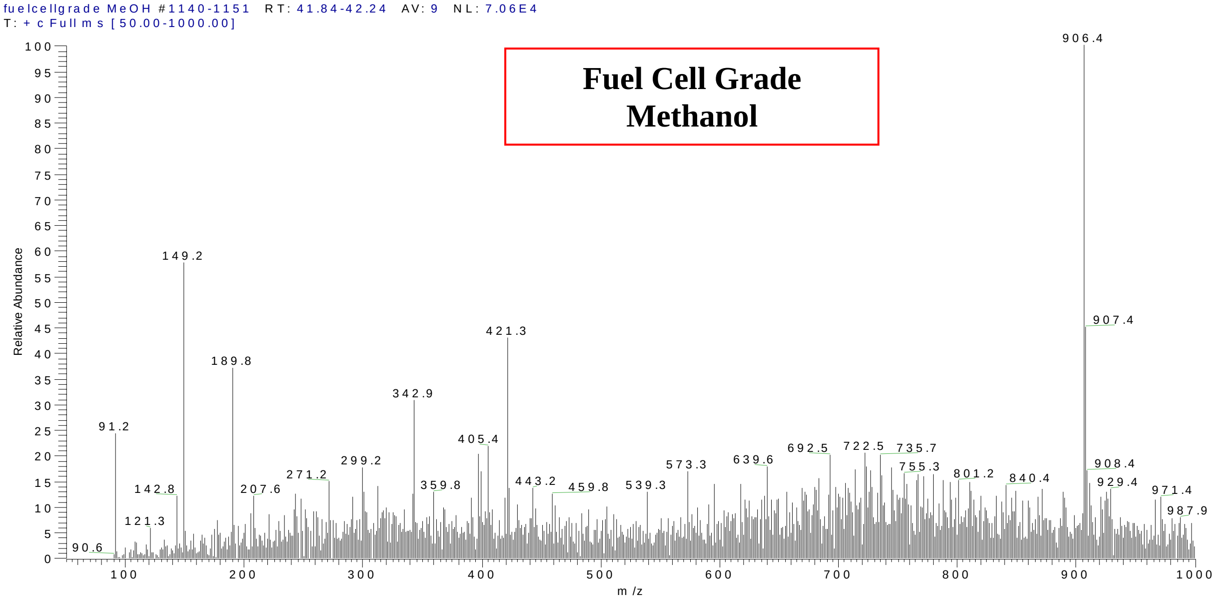

Figure 33: Mass Spectrograph for Fuel Cell Grade Methanol from 41min84sec to 42min24sec

In figure 32 and 33, two compounds have same base peak 906.4 and mass fragment patterns and running time. Two higher hydrocarbons which have approximately 929.4~ 971.4 g/mol molecular weight are identical.

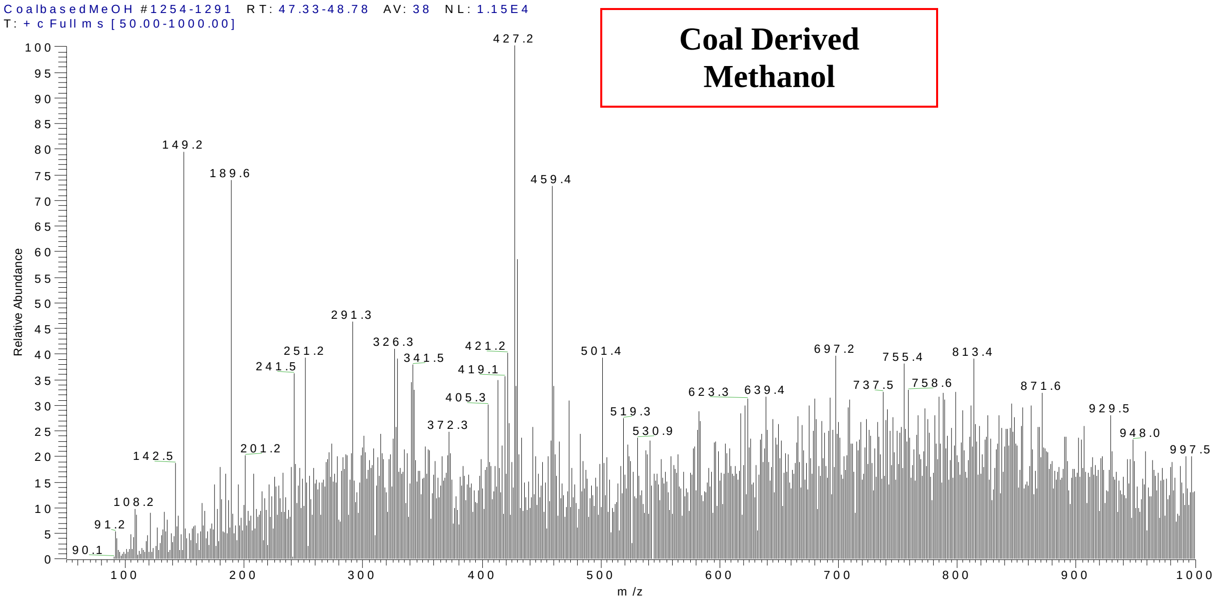

Figure 34: Mass Spectrograph for Coal-derived Methanol from 47min33sec to 48min78sec

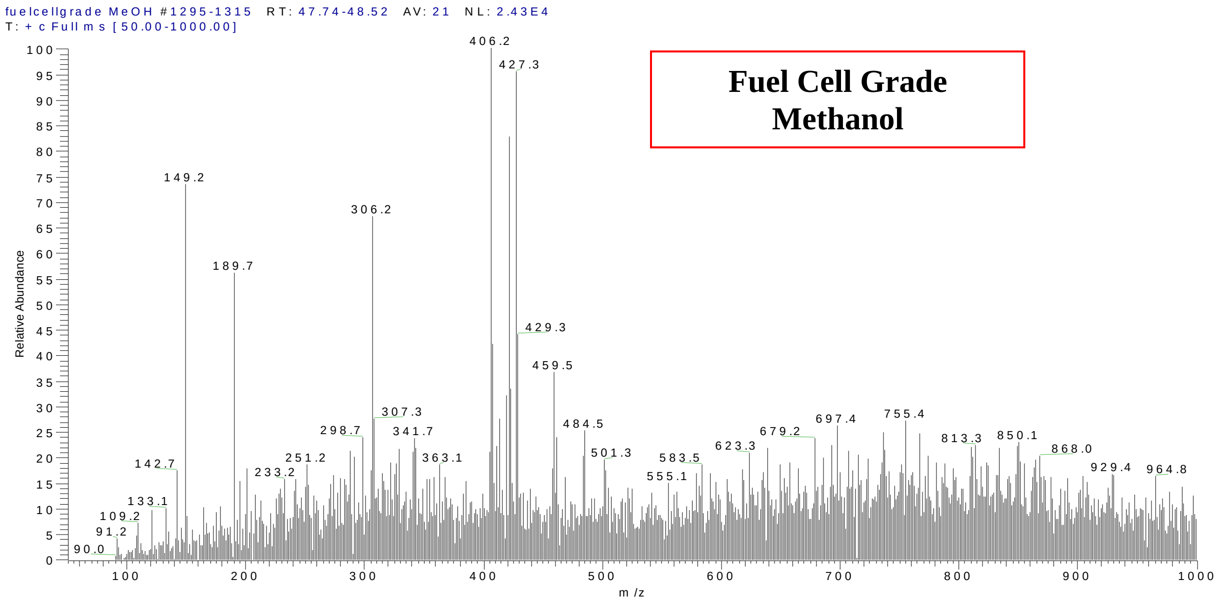

Figure 35: Mass Spectrograph for Fuel Cell Grade Methanol from 47min74sec to 48min52sec

Above two compounds are different because of different mass fragment patterns. In Figure 24 and 25, those graphs show different base peaks that one is 427.2 and another is 406.2. Both compounds can be hardly evaluated with regard to molecular weight due to noise

Consequently, there are lots of candidates spectrograph for above those higher hydrocarbon compounds corresponded by mass spectrograph. Obviously, coal-derived methanol and fuel cell grade methanol have in common with same higher hydrocarbons according to in case of figure 18 and 19, 20 and 21, 28 and 29, 32 and 33 except the others. Even though LC-MS results indicate there are difference between fuel cell grade methanol and coal-derived methanol, it is hardly possible to find out which compounds are in both methanol only using mass spectrograph.

Gas Chromatography-Mass spectrometer (GC-MS)

Figure 36 and 37 represent overall GC-MS time trace both coal-derived methanol and fuel cell grade methanol. What were found by GC-MS test were different types of higher hydrocarbon that some of them might have chloride, sulfur or silane.

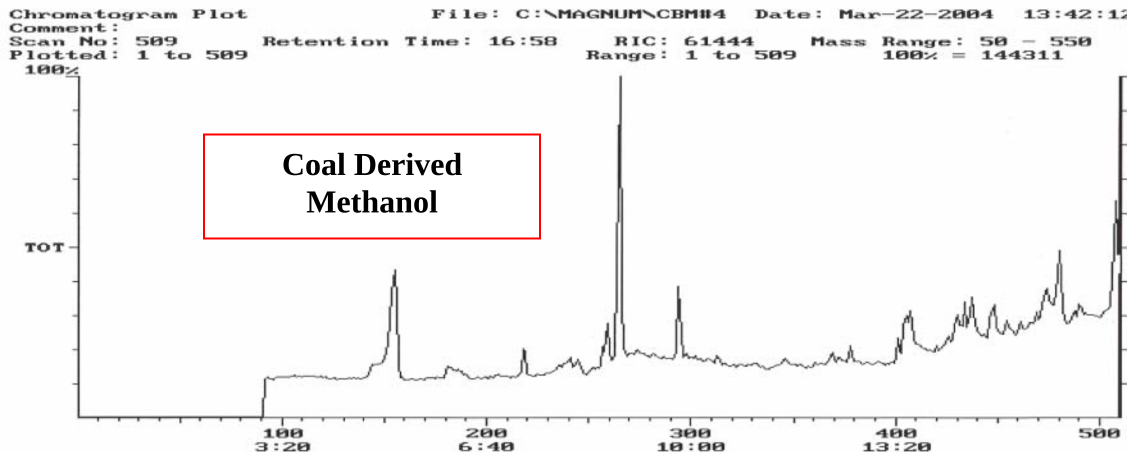

Figure 36: GC-MS time trace of Coal-derived Methanol

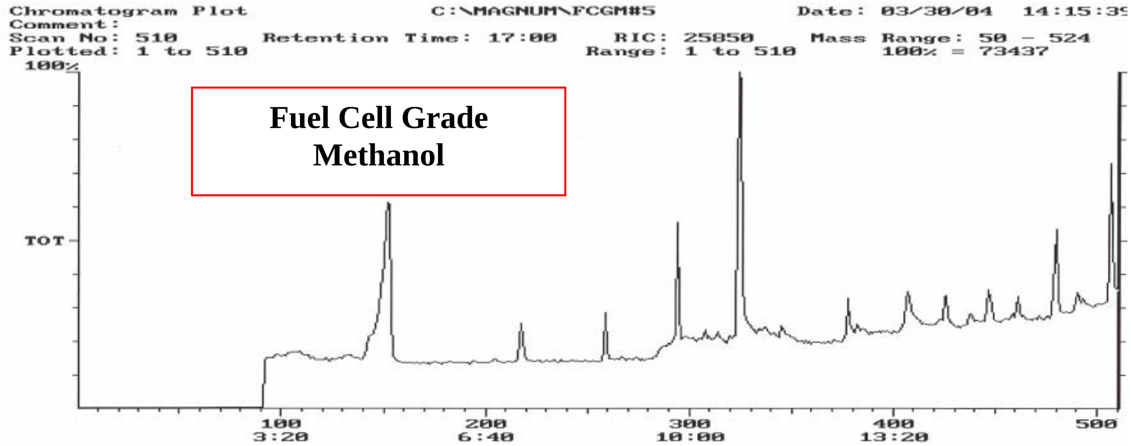

Figure 37: GC-MS time trace of Fuel Cell Grade Methanol

Figure 36 and 37 show different GC-MS time trace of coal-derive methanol and fuel cell grade methanol. Note Followed results with regard to mass spectrometer are based on GC-MS library.

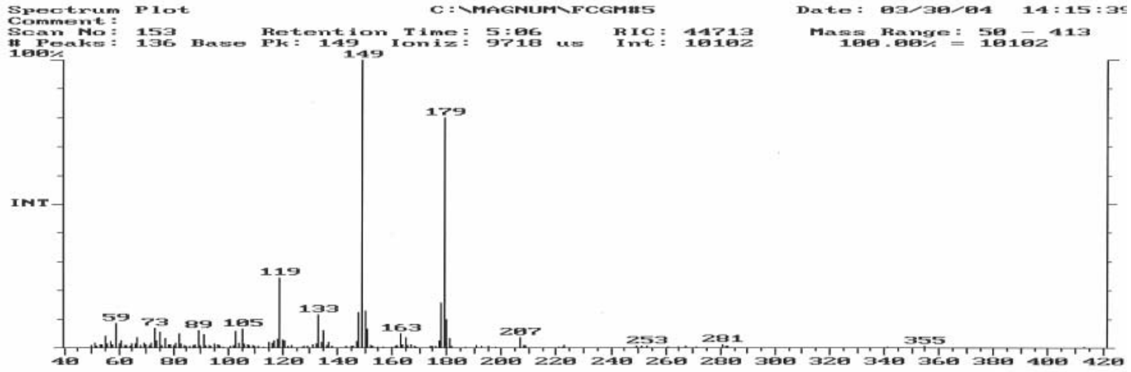

Figure 38: Mass spectrograph of Fuel Cell Grade Methanol at retention time 5:06

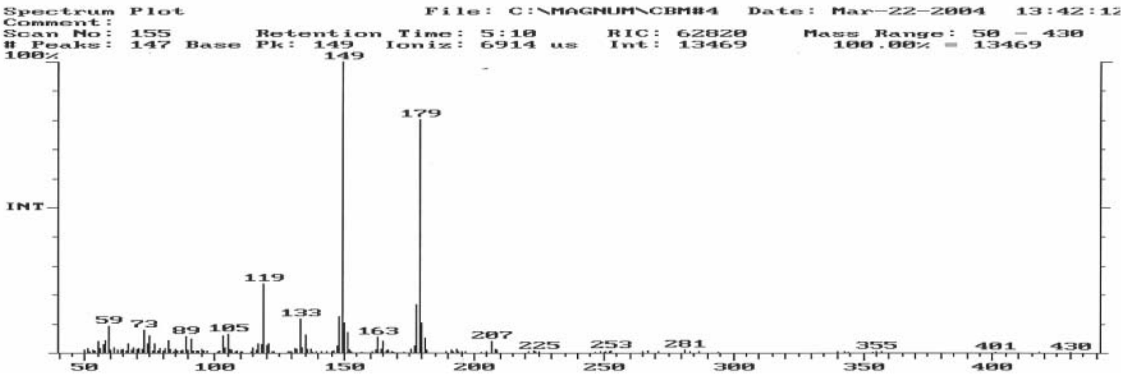

Figure 39: Mass spectrograph of Coal-derived Methanol at retention time 5:10

In figure 38 and 39, two compounds has 296 g/mol molecular weight and possible molecular formula is $C_{14}H_{24}O_3Si_2$ - Benzeneacetic acid, .alpha.-[(trimethylsilyl) oxy]-,tri. in both fuel cell grade and coal-derived methanol.

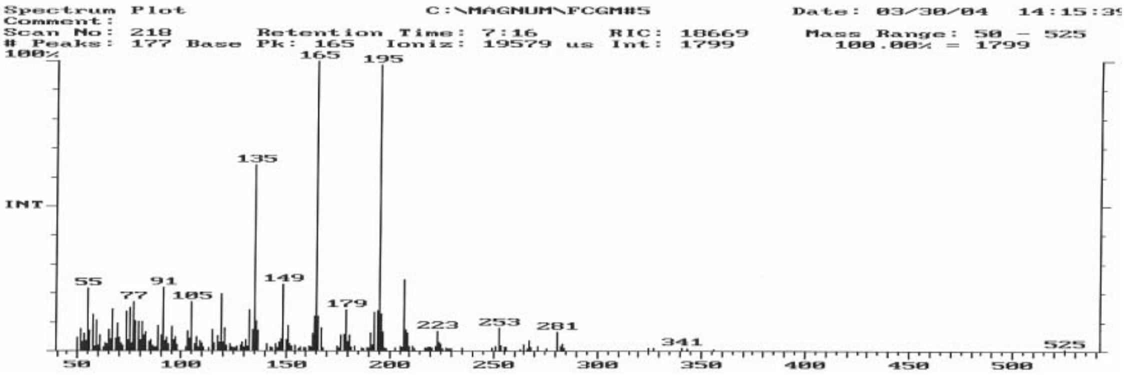

Figure 40: Mass spectrograph of Fuel Cell Grade Methanol at retention time 7:16

In figure 40, this compound has 268 g/mol molecular weight and possible molecular formula is $C_{18}H_{20}O_2$ which is 1, 2-Naphtaleneidol, 1, 2, 3, 4-tetrahydro-3, 3-dimethyl-1

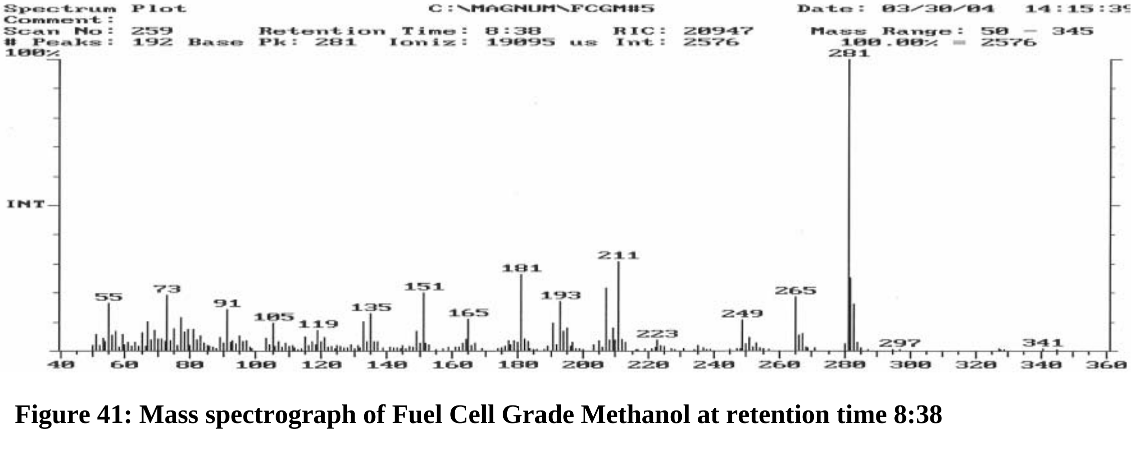

Figure 41: Mass spectrograph of Fuel Cell Grade Methanol at retention time 8:38

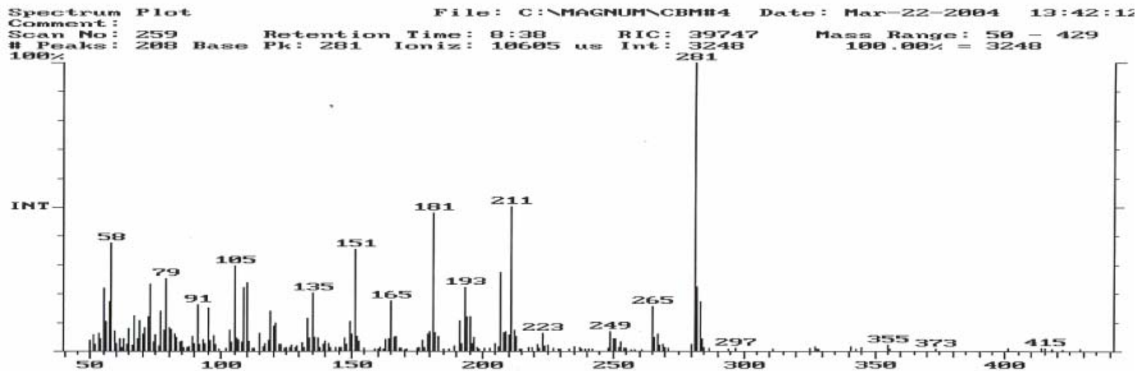

Figure 42: Mass spectrograph of Coal-derived Methanol at retention time 8:38

In figure 41 and 42, this compound has 296 g/mol molecular weight and possible molecular formula is $C_8H_{24}O_4Si_4$ -Cyclotetrasiloxane, octamethyle in both fuel cell grade and coal-derived methanol.

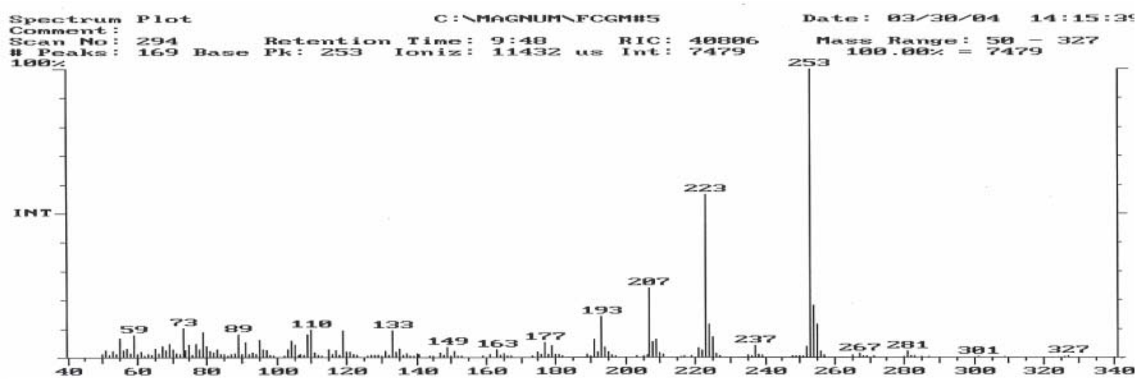

Figure 43: Mass spectrograph of Fuel Cell Grade Methanol at retention time 9:40

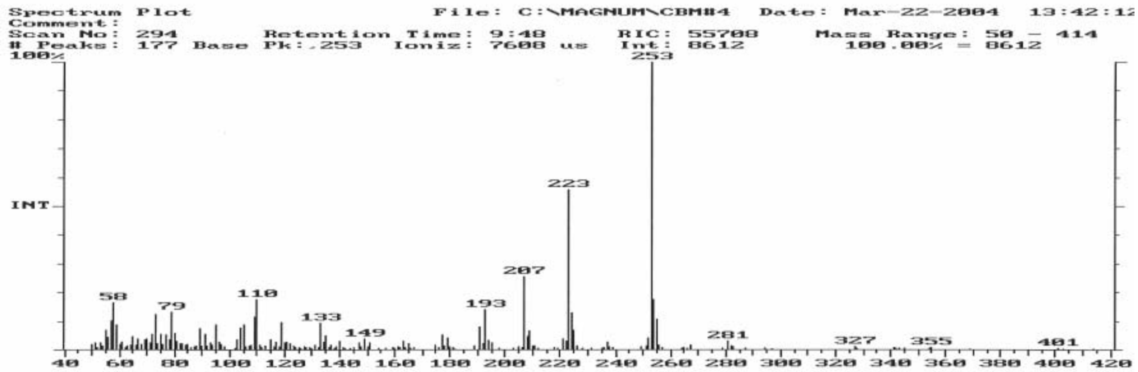

Figure 44: Mass spectrograph of Fuel Cell Grade Methanol at retention time 9:40

In figure 43 and 44, two compounds have same 253 g/mol molecular weight and possible molecular formula is $C_{12}H_{19}NO_3Si$ -Benzaldehyde, 3-methoxy-4-[tyimethylsily]oxy]. in both fuel cell grade and coal-derived methanol.

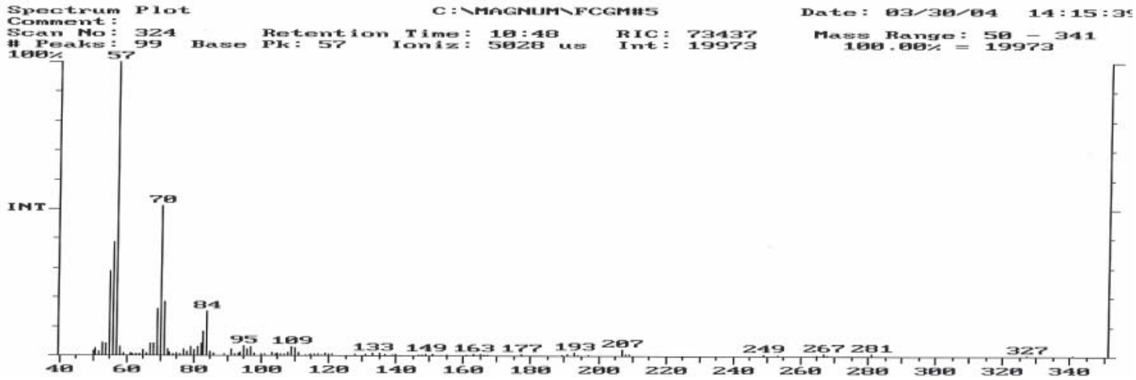

```
Spectrum Plot                  C:\MAGNUM\FCGM#5            Date: 03/30/04   14:15:3
Comment:
Scan No: 324         Retention Time: 10:48     RIC: 73437      Mass Range: 50 - 341
# Peaks: 99   Base Pk: 57     Ioniz: 5028 us   Int: 19973        100.00% = 19973
```

Figure 45: Mass spectrograph of Fuel Cell Grade Methanol at retention time 7:16

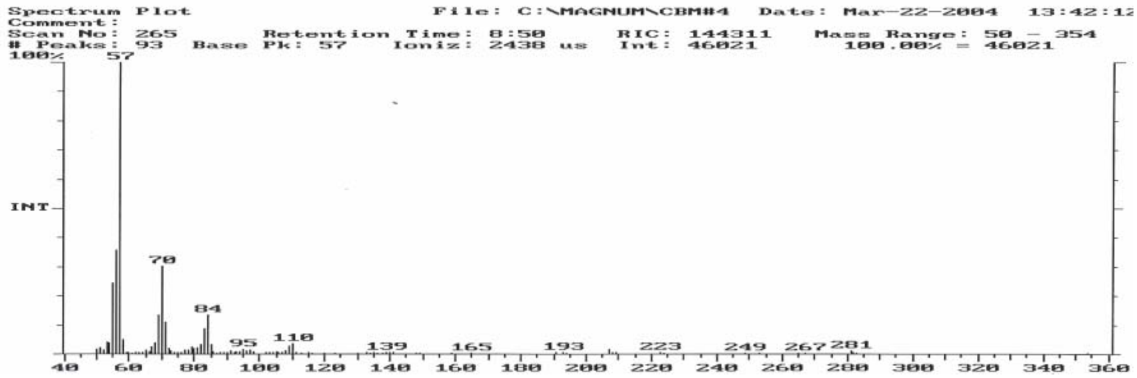

```
Spectrum Plot              File: C:\MAGNUM\CBM#4   Date: Mar-22-2004   13:42:1
Comment:
Scan No: 265         Retention Time: 8:50      RIC: 144311     Mass Range: 50 - 354
# Peaks: 93   Base Pk: 57     Ioniz: 2438 us   Int: 46021        100.00% = 46021
```

Figure 46: Mass spectrograph of Coal-derived Methanol at retention time 8:58

In figure 45 and 46, two compounds have 142 g/mol molecular weight and possible compounds are $C_{12}H_{25}F$ Dodecane-1-fluoro in both fuel cell grade and coal-derived methanol.

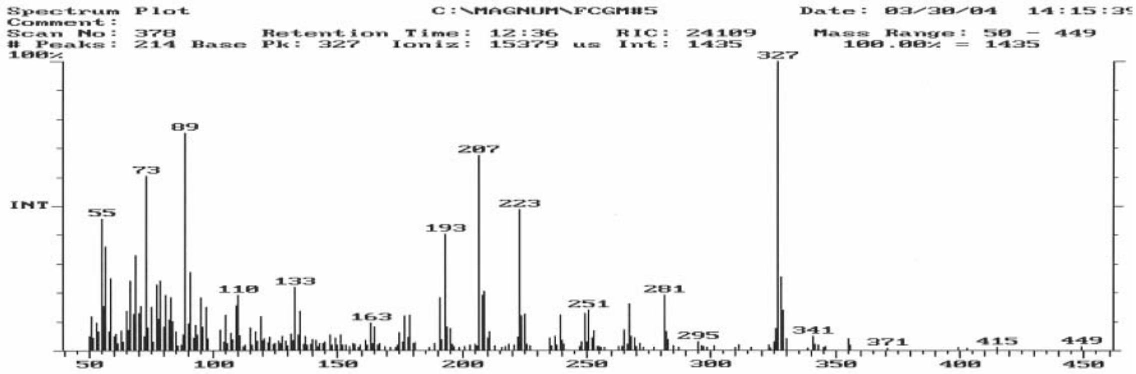

```
Spectrum Plot                  C:\MAGNUM\FCGM#5            Date: 03/30/04   14:15:3
Comment:
Scan No: 378         Retention Time: 12:36     RIC: 24109      Mass Range: 50 - 449
# Peaks: 214  Base Pk: 327    Ioniz: 15379 us  Int: 1435         100.00% = 1435
```

Figure 47: Mass spectrograph of Fuel Cell Grade Methanol at retention time 12:36

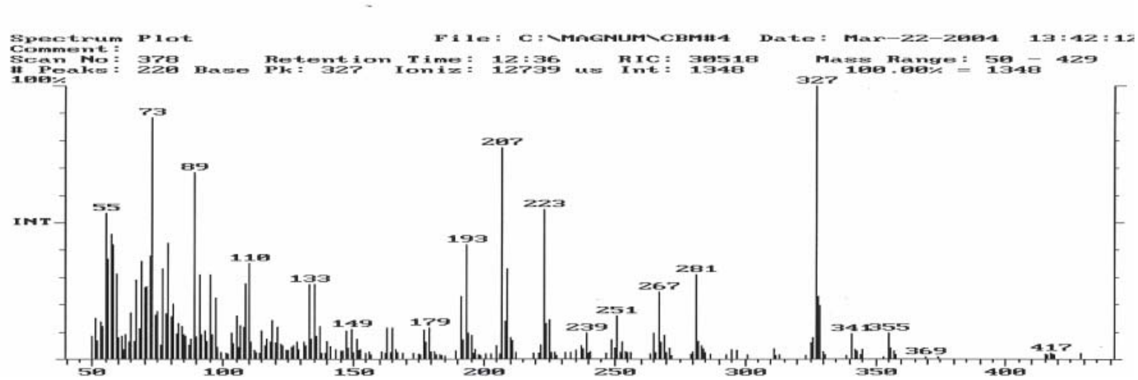

Figure 48: Mass spectrograph of Coal-derived Methanol at retention time 12:36

In figure 47 and 48, this compound has 342 g/mol molecular weight and possible molecular compounds is $C_9H_{30}O_4Si_5$ -1,1,1,3,4,7,9,9,9-Nonamethylpentasiloxane in both fuel cell grade and coal-derived methanol.

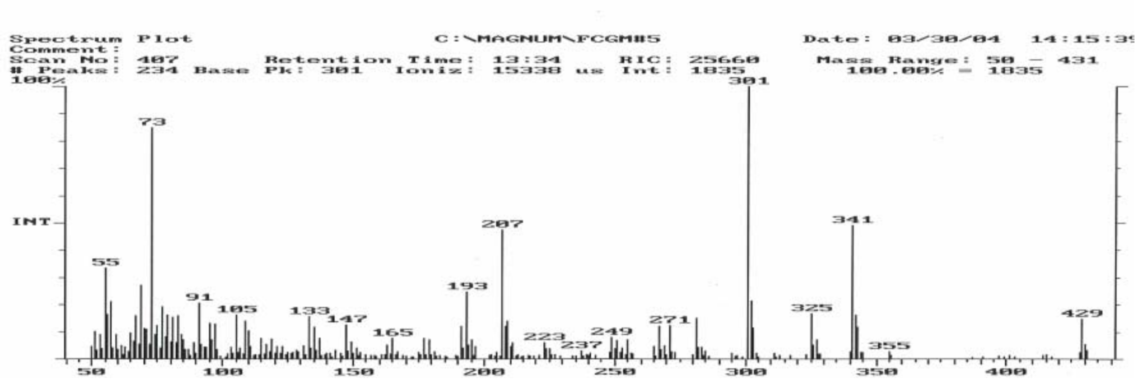

Figure 49: Mass spectrograph of Fuel Cell Grade Methanol at retention time 13:34

In figure 49, this compound has 444 g/mol molecular weight and possible molecular compounds is $C_{12}H_{36}O_6Si_6$ -cyclohexasiloxane, dodecamethyl in fuel cell grade.

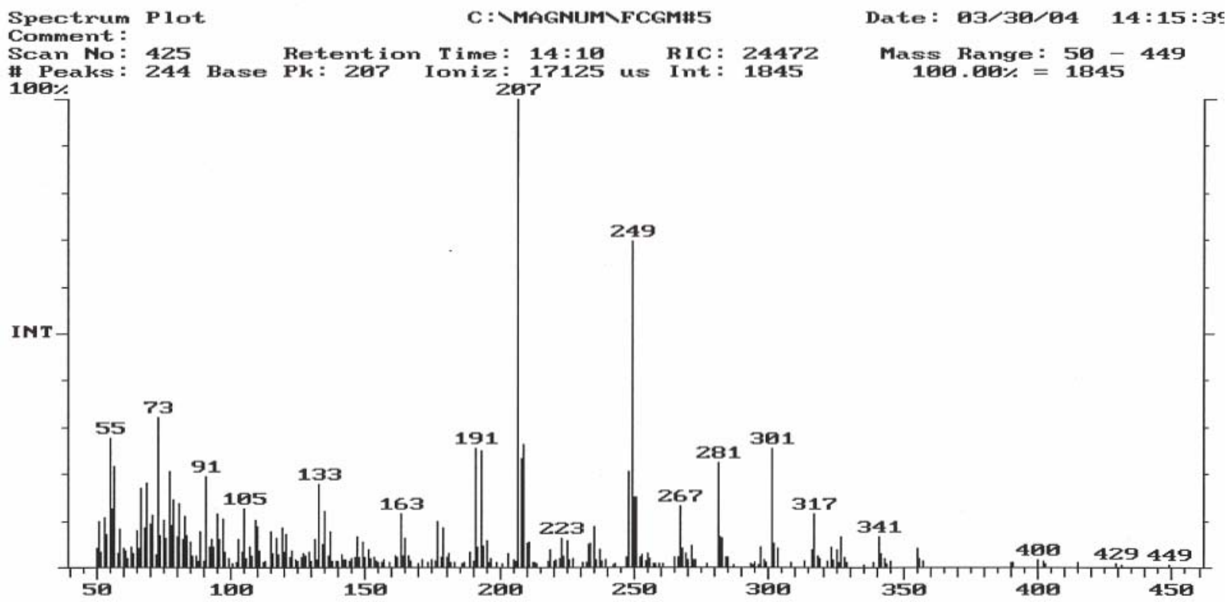

```
Spectrum Plot                  C:\MAGNUM\FCGM#5           Date: 03/30/04   14:15:3
Comment:
Scan No: 425       Retention Time: 14:10     RIC: 24472      Mass Range: 50 - 449
# Peaks: 244 Base Pk: 207   Ioniz: 17125 us Int: 1845          100.00% = 1845
```

Figure 50: Mass spectrograph of Fuel Cell Grade Methanol about retention time 14:10

In figure 50, this compound has 296 g/mol molecular weight and possible molecular compounds is $C_8H_{24}O_4Si_4$ -cyclotetrasiloxane, octamethly- in fuel cell grade and coal-derived methanol.

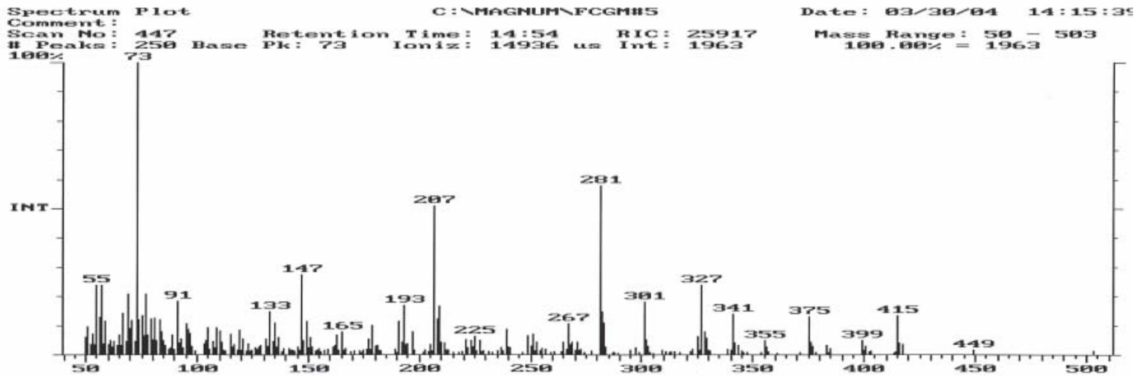

```
Spectrum Plot                  C:\MAGNUM\FCGM#5           Date: 03/30/04   14:15:3
Comment:
Scan No: 447       Retention Time: 14:54     RIC: 25917      Mass Range: 50 - 503
# Peaks: 250 Base Pk: 73    Ioniz: 14936 us Int: 1963          100.00% = 1963
```

Figure 51: Mass spectrograph of Fuel Cell Grade Methanol at retention time 14:54

In figure 51, this compound has 342 g/mol molecular weight and possible molecular compounds is $C_9H_{30}O_4Si_5$ -1,1,1,3,4,7,9,9,9-Nonamethylpentasiloxane in fuel cell grade

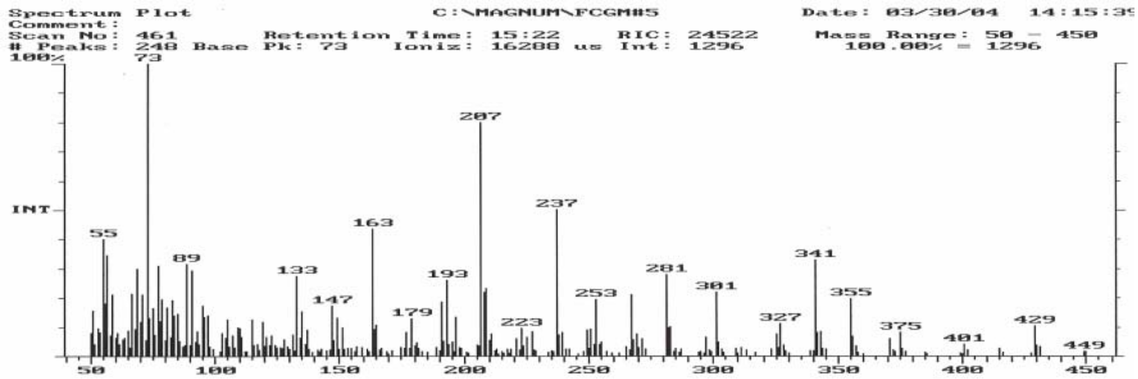

Figure 52: Mass spectrograph of Fuel Cell Grade Methanol at retention time 15:22

In figure 52, this compound has 296 g/mol molecular weight and possible formula is $C_{10}H_{28}O_4Si_3$ -3,3-Diethoxy-1,1,1,5,5,5-hexamethyltrisiloxane in fuel cell grade methanol.

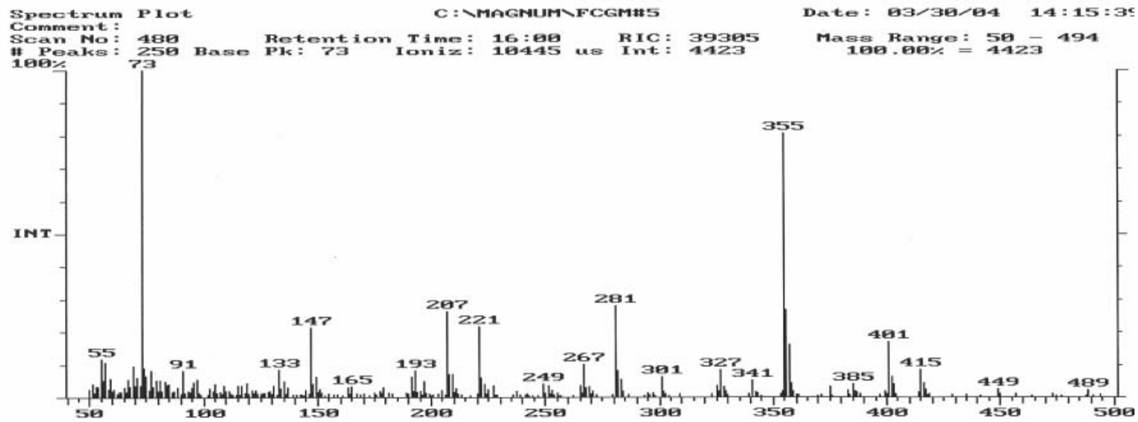

Figure 53: Mass spectrograph of Fuel Cell Grade Methanol at retention time 16:00

In figure 53, this compound has 370 g/mol molecular weight and possible formula is $C_{16}H_{30}O_4Si_3$-Benzoic acid, 2,4-bis[(trimethylsily)oxy]-trimethyls in fuel cell grade methanol.

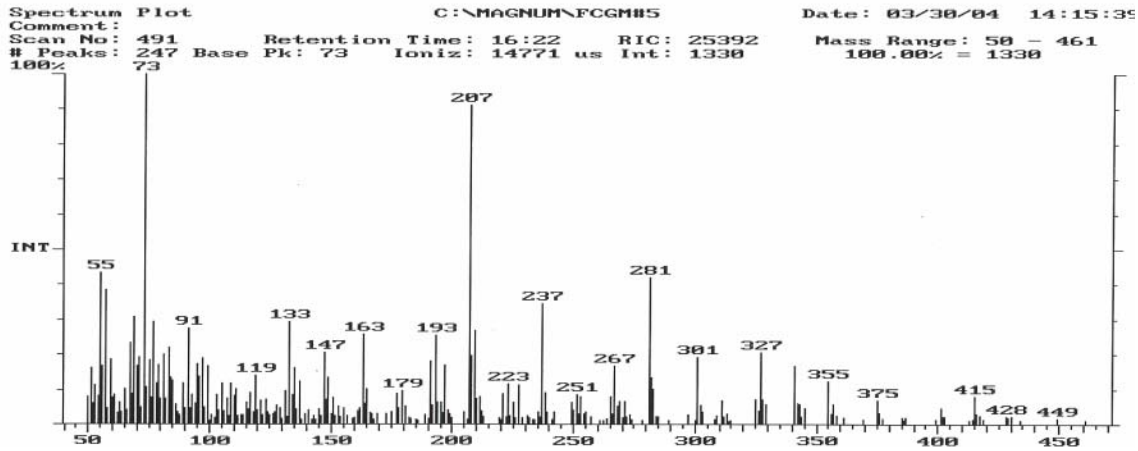

Figure 54: Mass spectrograph of Fuel Cell Grade Methanol at retention time 16:22

In figure 54, this compound has 296 g/mol molecular weight and possible formula is $C_{10}H_{28}O_4Si_3$ -3,3-Diethoxy-1,1,1,5,5,5-hexamethyltrisiloxane in fuel cell grade methanol.

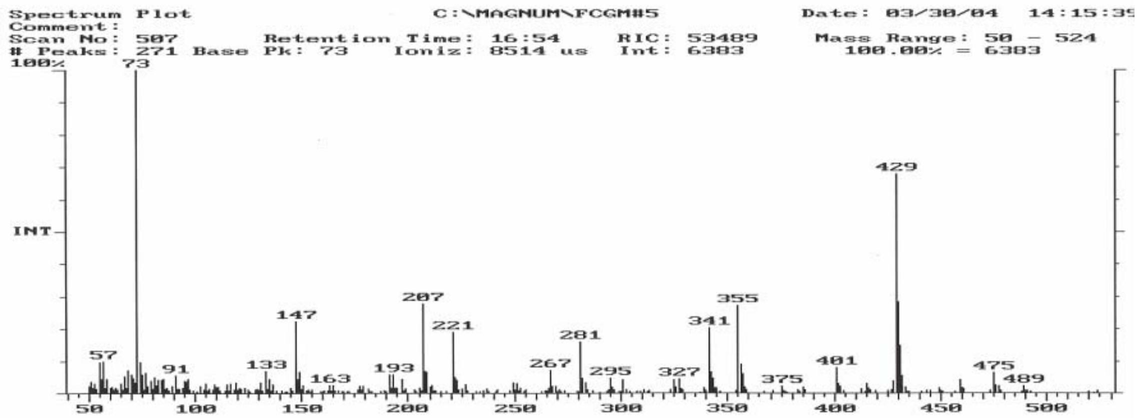

Figure 55: Mass spectrograph of Fuel Cell Grade Methanol at retention time 16:54

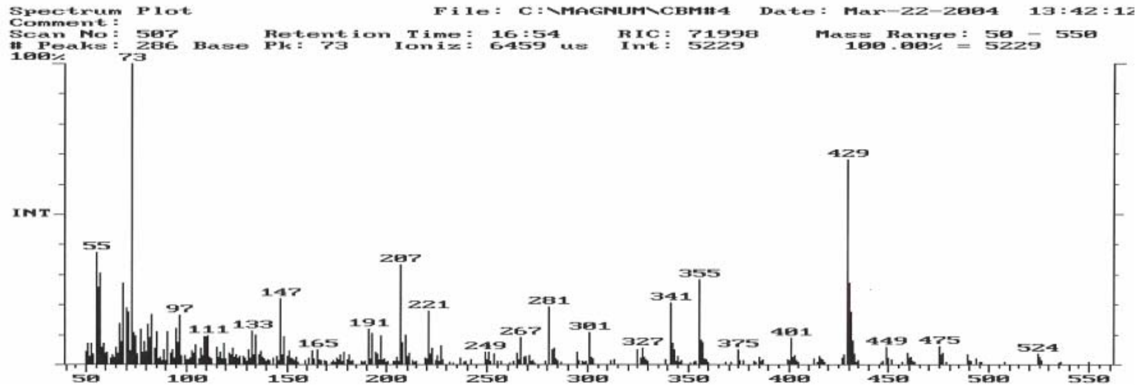

Figure 56: Mass spectrograph of Coal-derived Methanol at retention time 16:54

In figure 55 and 56, two compounds have 444 g/mol molecular weight and possible formula is $C_{13}H_{40}O_5Si_6$-1,1,1,5,7,7,7-Heptamethyl-3,3-bis(trimethylsiloxy)tetra in fuel cell grade and coal-derived methanol.

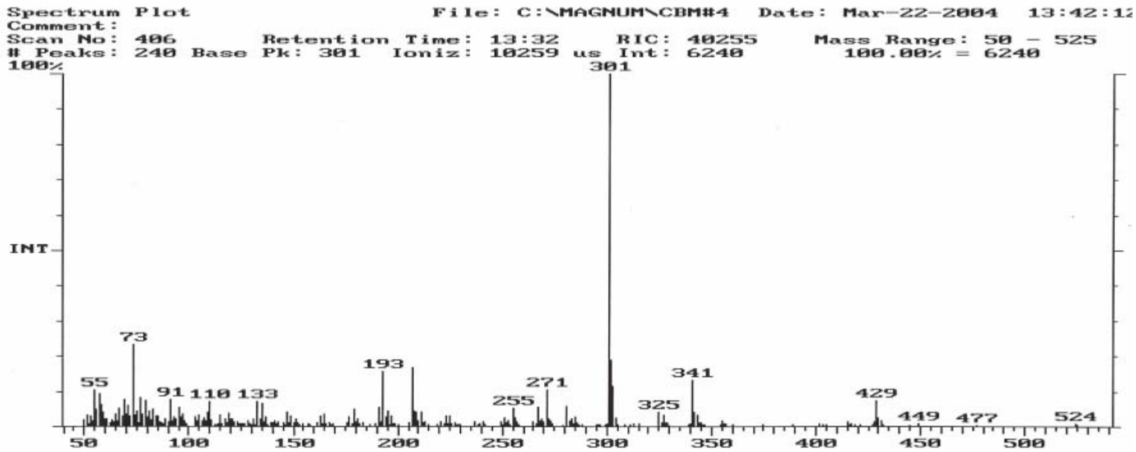

Figure 57: Mass spectrograph of Coal-derived Methanol at retention time 13:32

In figure 57, this compound has 301 g/mol molecular weight and possible formula is $C_3H_4F_5NS$ -2-pentafluorophenylbenzothiazole in coal-derived methanol.

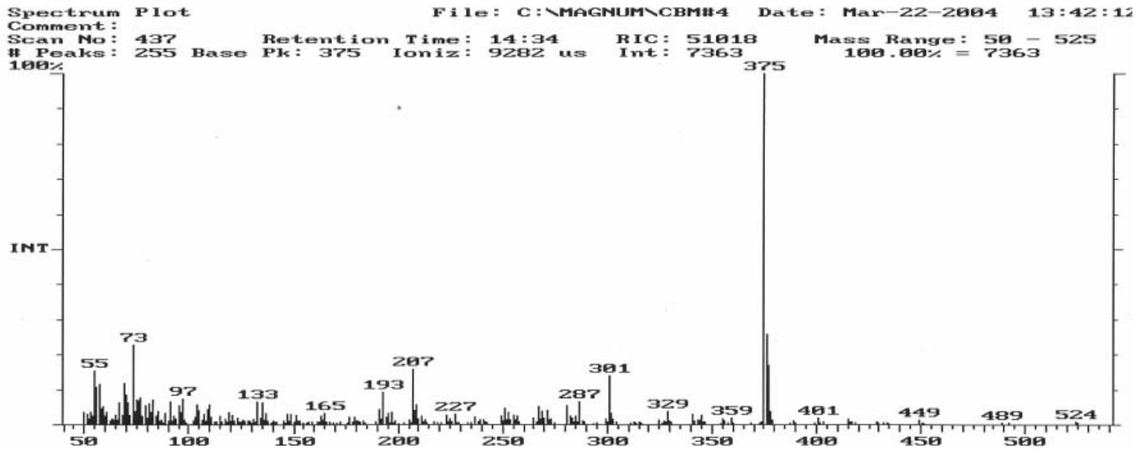

Figure 58: Mass spectrograph of Coal-derived Methanol at retention time 14:34

In figure 58, this compound has 404 g/mol molecular weight and possible formula is $C_{25}H_{44}O_2Si$ -Androstan-17-one, 3-[(triethylsilyl)oxy]-(3.beta.,5.a) in coal-derived methanol.

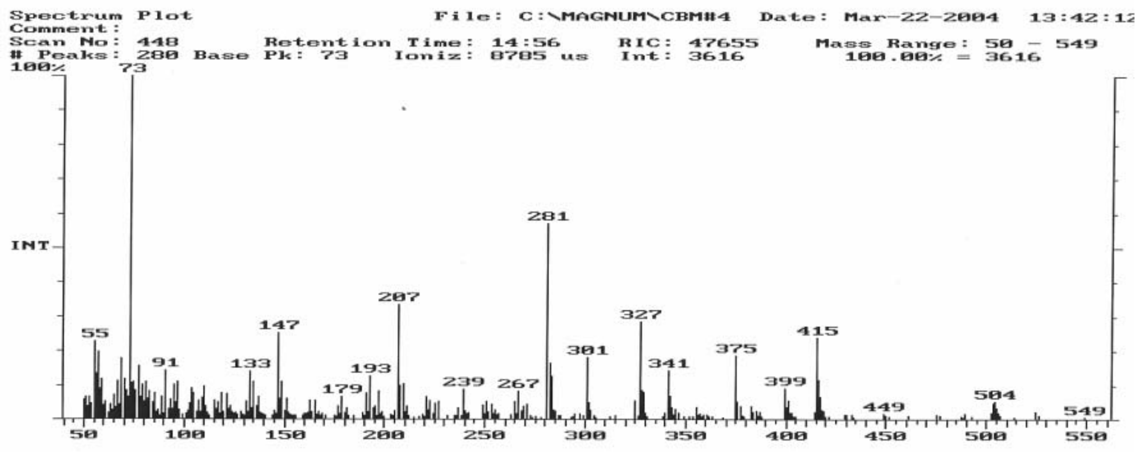

Figure 59: Mass spectrograph of Coal-derived Methanol at retention time 14:56

In figure 59, this compound has 342 g/mol molecular weight and possible molecular compounds is $C_9H_{30}O_4Si_5$ -1,1,1,3,4,7,9,9,9-Nonamethylpentasiloxane in coal-derived methanol.

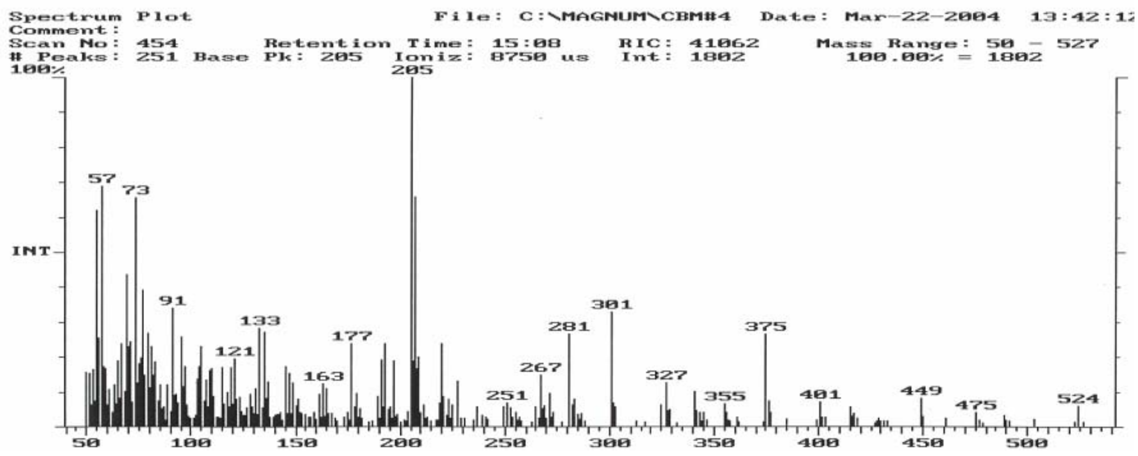

Figure 60: Mass spectrograph of Coal-derived Methanol at retention time 15:08

In figure 60, this compound has 262 g/mol molecular weight and possible molecular formula is $C_{17}H_{26}O_2$ -7,9-Di-t-buty1-1-oxaspiro[4,5]betadeca-6,9-dien-8-one.

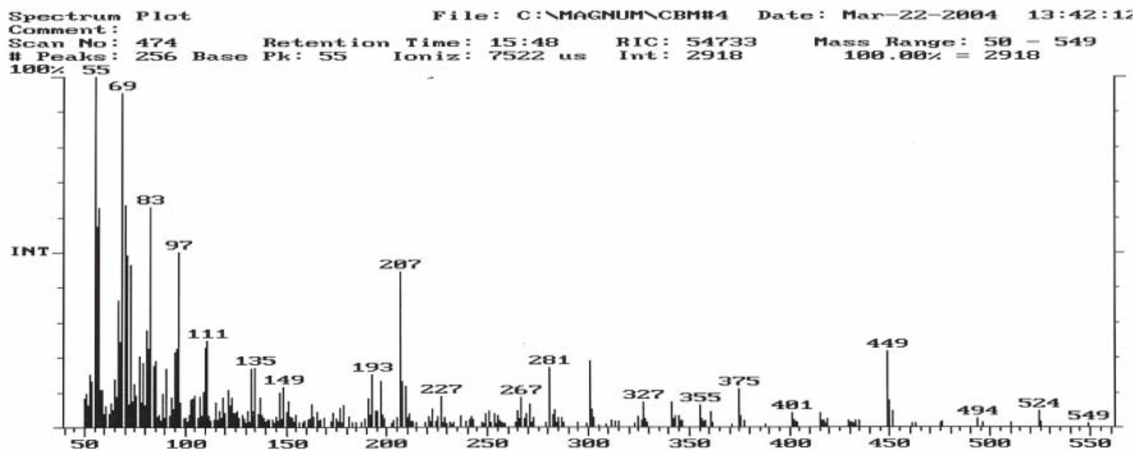

Figure 61: Mass spectrograph of Coal-derived Methanol at retention time 15:48

In figure 61, this compound has 268 g/mol molecular weight and possible molecular formula is $C_{13}H_{22}N_2O_2$. –Acetamide, N-methyl-[4-[4-methoxy-1-hexahydropyridyl] in coal-derived methanol.

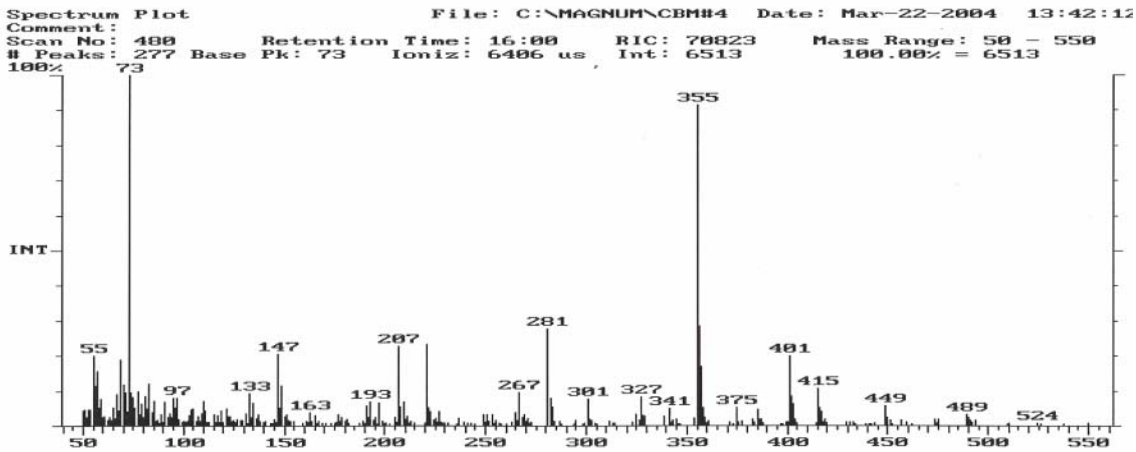

Figure 62: Mass spectrograph of Coal-derived Methanol at retention time 16:08

In figure 62, this compound has 296 g/mol molecular weight and possible molecular formula is $C_{10}H_{28}O_4Si_3$ 3,3-diethoxy-1,1,1,5,5,5-hexamethyltrisiloxane in coal-derived methanol.

Consequently, we considerably certified the difference of fuel cell grade methanol and coal-derived methanol through GC-MS. From figure 38 to 48, 55 and 56 those are identical hydrocarbon compounds. Although some compounds have same molecular weight through GC-MS library, they can not be said identical compounds because of different mass fragment patterns. However, most hydrocarbon compounds found by GC-MS library have silane which is abundant in the earth. Further research should be required because those silane might be sulfur, chloride or just column bleed. Further more, internal evaluation followed by ASTM standard is being on process to completely grasp coal-derived methanol specification.

Preliminary Results from Steam Reformation of Fuel Cell Grade Methanol

Table 2 shows raw data from a preliminary run of the steam reformer using fuel cell grade methanol. The premix density, condensate density, mass of premix used, and the mass of the condensate were reduced using the method described above to determine the percent conversion of methanol.

Table 2: Preliminary results from steam reformation of fuel cell grade methanol

	Premix Flow Rate (mL/min)	Premix Density (g/cm^3)	Mass of Premix Used (g)	Mass of Condensate (g)	Condensate Density (g/cm^3)	Percent Conversion (%)
Run 1	15	0.9080	208.2	38.6	0.9953	99.56
Run 2	5	0.9080	205.8	38.9	0.9973	99.93
Run 3	15	0.9080	208.4	34.5	0.9965	99.81
Run 4	15	0.9080	207.9	38.0	0.9969	99.86
Run 5	5	0.9080	205.7	37.0	0.9972	99.91
Run 6	5	0.9080	205.8	35.5	0.9973	99.93

Preliminary Results from Steam Reformation of Coal-Derived Methanol

Preliminary evaluation from steam reformation via coal-derived methanol has been accomplished. As mentioned by previous progress report, the catalyst used in this experiment was a pelletized commercial-grade copper-zinc catalyst on an alumina and graphite substrate. This catalyst (FCRM-2) was manufactured by Sud-Chemie and is recommended for an operating temperature range of 250-280^{o}C (482-536^{o}F). The catalyst was cylindrical in shape and had dimensions consisting of 0.47 cm (0.187 in)-diameter and 0.25 cm (0.100 in)-thickness, as stated by the manufacturer. The catalyst in its original state is referred to in this study as pelletized catalyst. The reactor A reported by first progressive report was used for this experiment. Table 3 shows random run order associated with premix flow rate, premix density, mass of premix used, mass of condensate and condensate density at 24°C.

Table 3: Preliminary results from steam reformation of coal-derived methanol

	Premix Flow Rate (mL/min)	Premix Density (g/cm^3)	Mass of Premix Used (g)	Mass of Condensate (g)	Condensate Density (g/cm^3)
Run 1	5	0.9081	211.2	38.9	0.996
Run 2	7.5	0.9081	211.1	40.6	0.9937
Run 3	15	0.9081	213.6	53.7	0.9718

Run 4	15	0.9081	210.6	52.9	0.9711
Run 5	5	0.9081	209.5	37.9	0.995
Run 6	7.5	0.9081	210.5	41.1	0.9919
Run 7	7.5	0.9081	218.3	43.2	0.9925
Run 8	5	0.9081	209.5	39.2	0.995
Run 9	15	0.9081	210.1	57.7	0.9674

Table4 represents average conversion ratio based on table 3 data as well as liquid hourly space velocity of methanol.

Table 4: Average conversion ratio associated with liquid hourly space velocity of methanol

Flow Rate (ml/min)	Total Flow Rate (g/min)	MeOH Flow Rate (m3/hr)	Run I	Run II	Run III	Avg.Conver. Ratio(%)	LHSV-M
5	4.5405	0.000187748	99.98	99.76	99.75	99.83	1.02
7.5	6.81075	0.000281622	99.44	99.01	99.14	99.20	1.53
10	9.081	0.000375496	98.84	98.47	98.64	98.65	2.05
15	13.6215	0.000563245	92.78	92.58	92.76	92.71	3.07
20	18.162	0.000750993	89.53	89.79	88.86	89.39	4.09

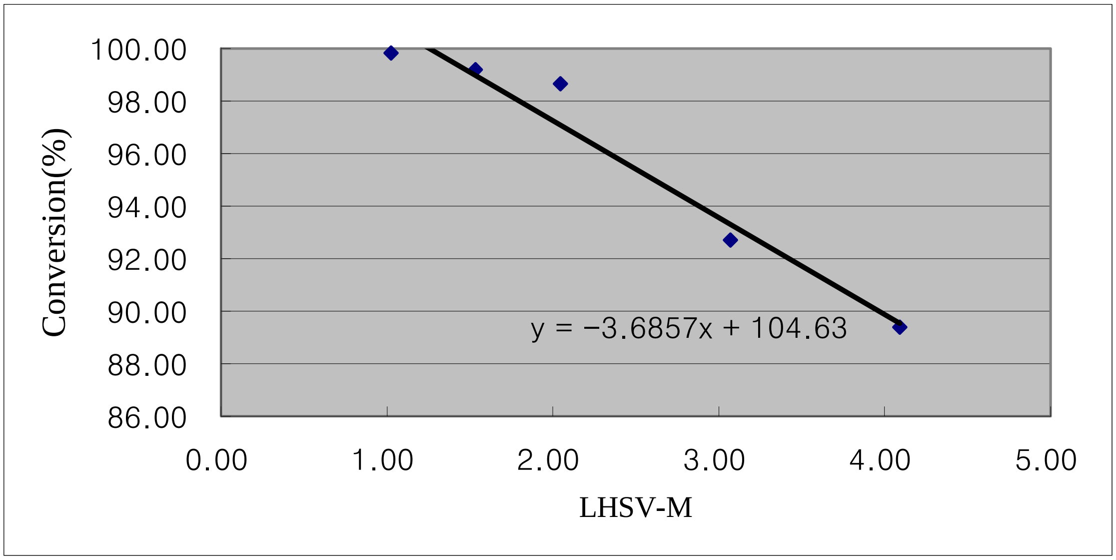

Figure 63: LHVS-M versus percent conversion

Figure 64 represents temperature profiles of the reactor A with regard to different liquid hourly space velocity of methanol.

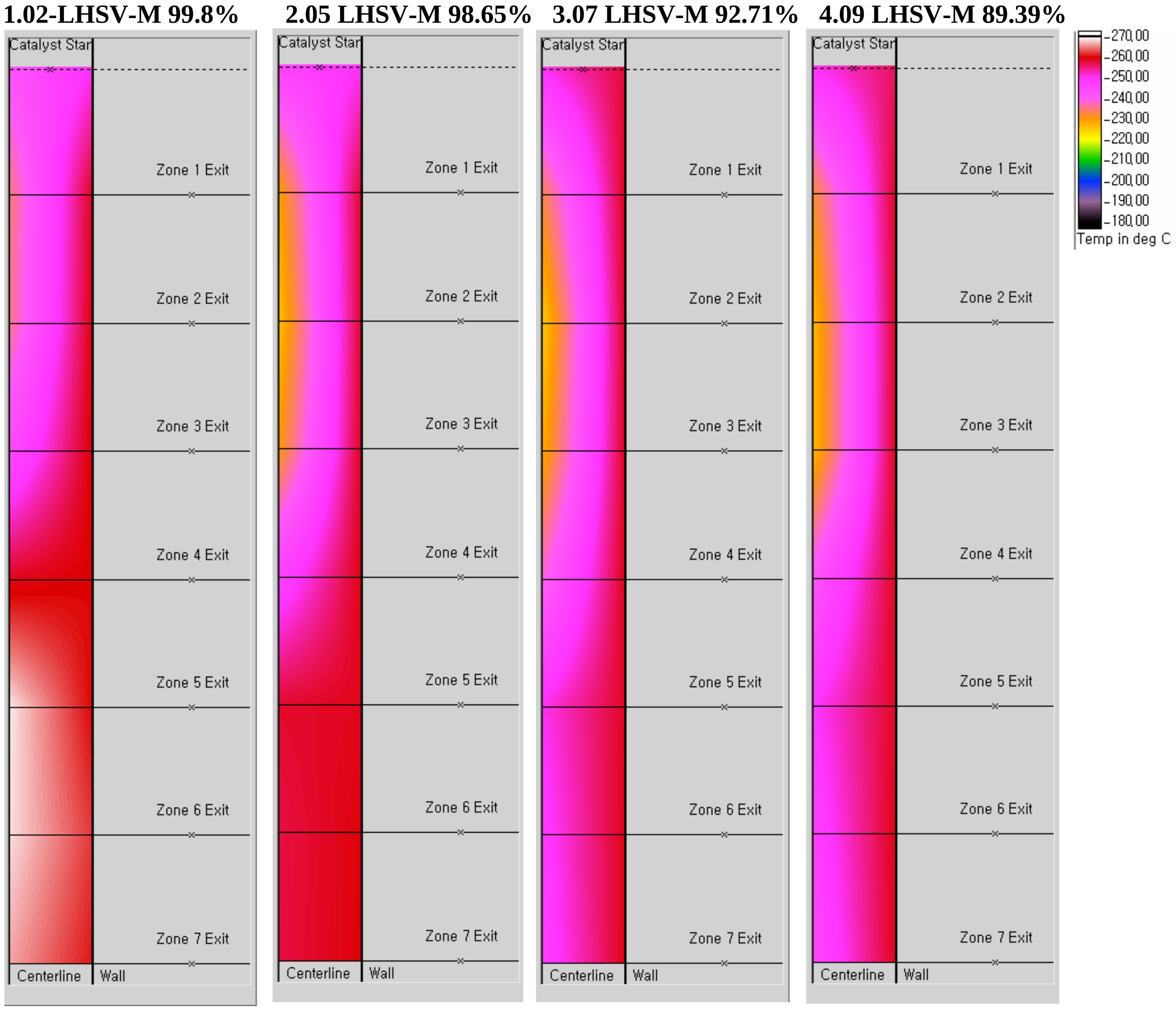
1.02-LHSV-M 99.8% 2.05 LHSV-M 98.65% 3.07 LHSV-M 92.71% 4.09 LHSV-M 89.39%

Figure 64: Temperature profile in the Reactor A

Hysteresis Tests using Coal-derived Methanol

Tests monitoring hydrogen production degradation were performed by using a hysteresis analysis using coal-derived methanol. Theoretically, catalyst degradation is unavoidable and strongly time-dependent. In this experiment, catalyst degradation as manifest by changes in conversion was monitored. This experiment was done in reactor A. The catalyst FCRM-2 manufactured by Sud-Chemie as mentioned above was used for this experiment. The pellitized catalyst which had been used for over 12 hours was tested for hysteresis in conversion. Initial flow rate was 5ml/min. The flowrate was increased to 10 ml/min, 15 ml/min and 20 ml/min respectively and went back to 5ml/min after each increase. Nominal time on-stream was approximately 30minutes at each flow rate. Conversion was calculated at each flow rate and these results are shown in Table 5 and graphically in Figure 65. In case of 5ml/min or 1.02 LHSV-M, conversion did not change significantly for these experiments. Further hysteresis tests will be performed leaving the reactor on stream for longer periods of time

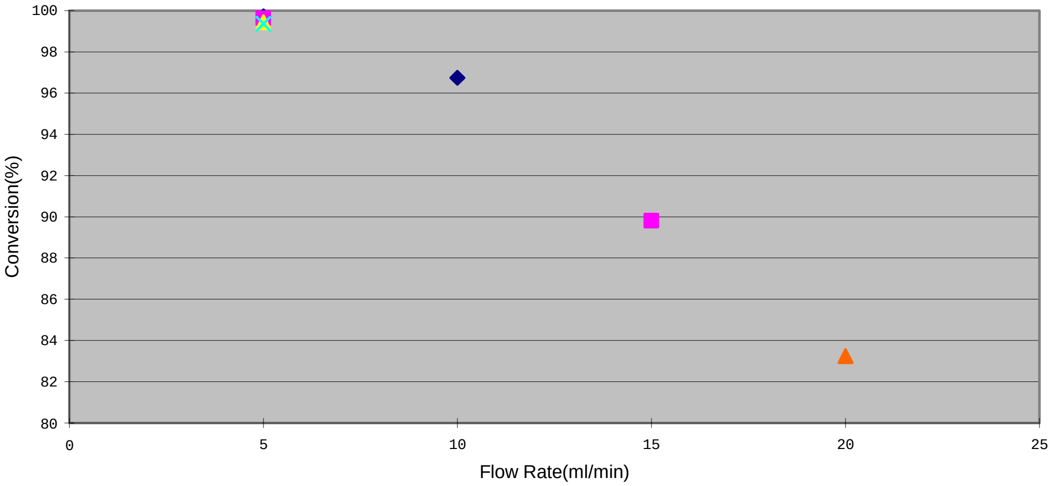

Figure 65: Results of hysteresis testing

Table 5: Results of hysteresis testing

Flow Rate (mL/min)	% Conversion of Methanol
5	99.73
10	96.74
5	99.62
15	89.81
5	99.36
20	83.25
5	99.44

Catalyst Degradation

Catalyst degradation research must be performed to validate the compatibility of coal-derived methanol with fuel cell applications. Copper based catalysts which have been used for this experiment can be deactivated by sulfur and chloride poisoning, thermal sintering, fouling (i.e. coke formation), and physical damage such as attrition caused by vibration and crushing. Furthermore, different phase reaction (i.e. vapor-solid reaction) might be responsible for catalyst degradation. [4], [5], [6], [7]. Some researchers suggest formation of formaldehyde as by-product might deactivate copper based catalysts. [6] Additionally, copper based catalyst without substrates show weakness in thermal sintering, fouling and physical damage. However, copper based catalysts with substrates and/or sacrificial elements can be resistive to the degradation causes mentioned above. For example, Zinc can remove sulfur by means of forming Zinc Sulfide to protect the copper catalyst.

External analysis of the coal derived methanol shows lower levels of sulfur, increased levels of petroleum hydrocarbons and extremely high chloride levels as compared to fuel cell grade methanol (see external methanol analysis section). The potential of coal based methanol as a source of hydrogen is dependant on the effect of these contaminants on the steam reformation catalyst. Catalyst degradation rates for fuel cell grade methanol and coal based methanol are being measured using the hysteresis technique (see hysteresis section). A comparison of the rates of degradation will determine the severity of the effect of the higher contaminant levels in the coal based methanol. In order to prioritize the importance of reducing specific kinds of contamination we must understand not only the total amount of catalyst degradation but also the type of degradation that is occurring categorized as poisoning, fouling and sintering. As discussed above poisoning of copper based catalysts can be caused by chloride and sulfur containing compounds. Fouling can be caused by condensation of low volatility hydrocarbons or by solid carbon deposition on catalyst surfaces. Sintering can be caused by hot spots and temperature gradients in the reactor. The catalyst degradation project aims to characterize the catalyst materials in order to develop a means of identifying the dominant type of degradation when using coal derived methanol. The first stage of the project has been to identify analytical techniques and tools to characterize the catalysts. The following list of techniques have been identified as potential candidates and are available on the UC Davis campus.

Analysis Techniques:

- SEM: Scanning Electron Microscopy to measure surface changes
- SEM/EDS: Electron Dispersive Spectroscopy to identify atomic species on the surface
- XRD: X-Ray Diffraction to identify solid solution alloy formation and to measure particle growth caused by sintering
- BET: to measure surface area which could be affected by sintering or fouling of the catalyst
- XPS: X-Ray Photoelectron Spectroscopy to identify and quantify the concentration of catalyst poisons in trace quantities on the catalyst surface
- Mercury Porosymetry: to measure pore volume and pore size distribution
- Light Microscopy: characterize surface

In the January 1st to March 31st time frame preliminary investigations were made using the Light Microscopy, Scanning Electron Microscopy, the Electron Dispersive Spectroscopy and the X-Ray Diffraction techniques. The investigations to date have focused on the CuO/ZnO/Graphite catalyst supplied by Sud Chemie due to its high activity and low operating temperature. The catalyst in the as received oxidized state has a black matte surface on the ends and a black shiny surface around the edges.

Figure 66: Sud Chemie pelletized FCRM-2 catalyst

Light microscopy results show that the surface is very rough with very small pores penetrating into the pellet, very reflective sections and regions of different colors. For reactor operation the catalyst is reduced and when removed from the reactor the catalyst reoxidizes in air heating up to 190°C. When the reduced catalyst is removed from the reactor it has a ruby sheen and then as it oxidizes the hottest sections of catalyst turn a pale green color. The difference between these two surfaces can be seen in the light microscope pictures below. Literature investigations suggest that this coloration change may only be related to the reoxidation conditions and may not be caused by chemical changes to the surface of the catalyst during opertation. Further work will focus on developing the infrastructure to analyze the catalyst in reduced form in order to make stronger comparisons.

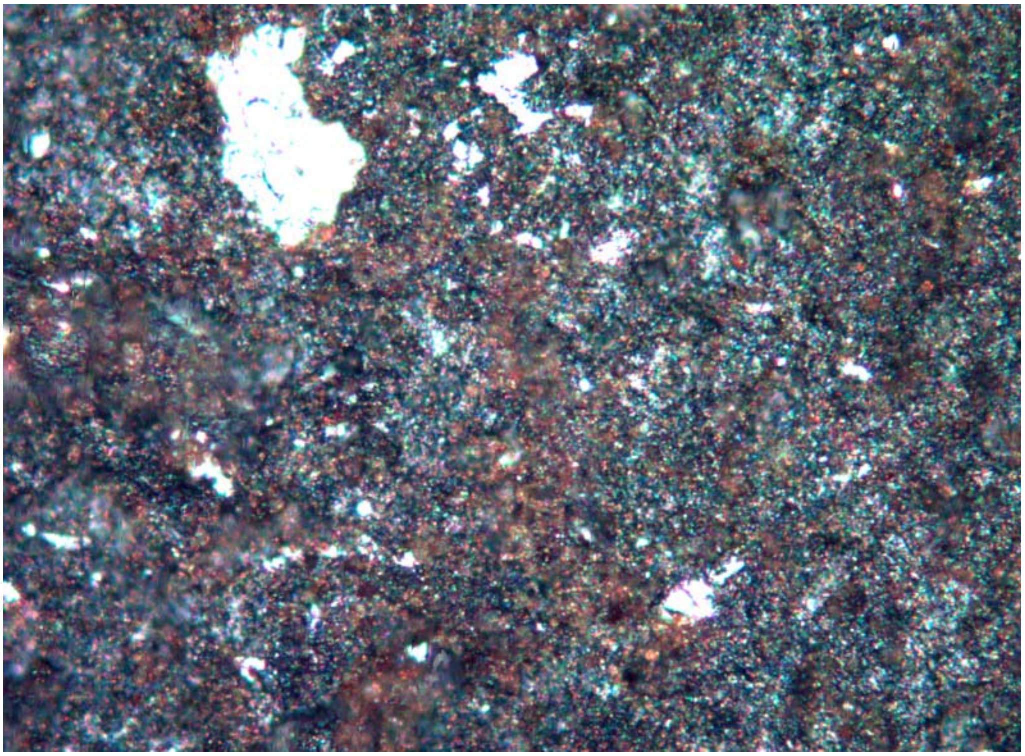

Figure 67: Virgin Catalyst surface at 400X magnification, Extended focal image composite of 5 images

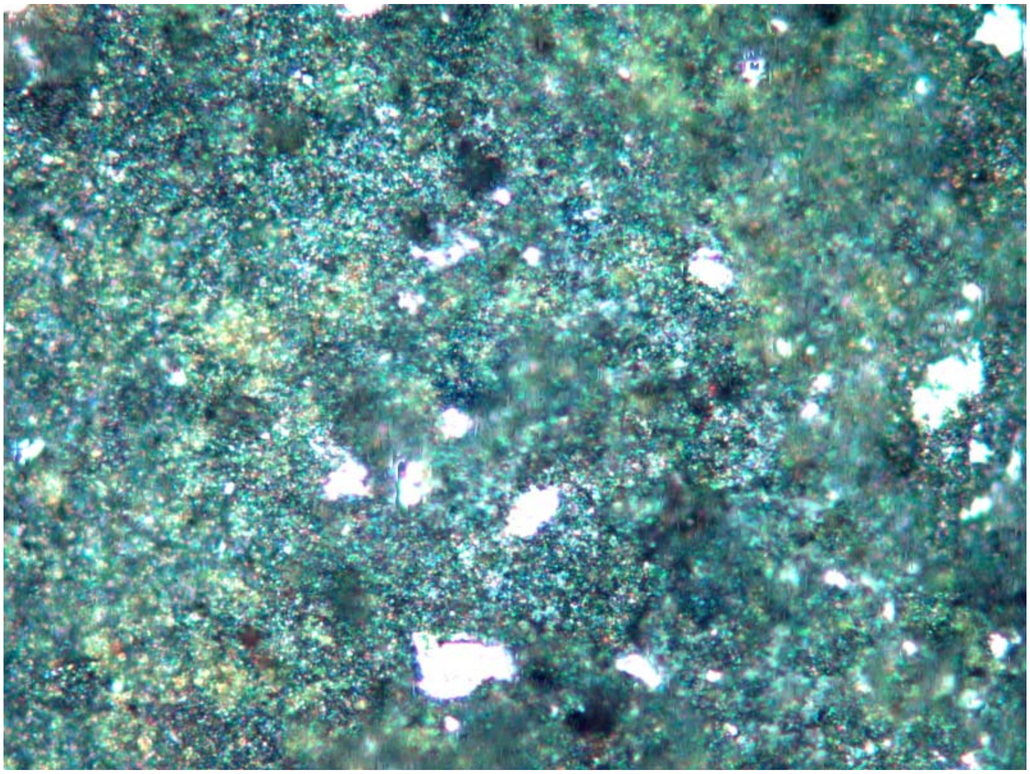

Figure 68: Used Oxidized Catalyst surface at 400X magnification, Extended focal image composite of 5 images

SEM microscopy results have determined that the catalyst particles are composed of consolidated fine particles with particles sizes on the order of nanometers. The catalyst pellets have very fine pore structures with pore diameters on the order of nanometers as well as the larger pores seen in the light microscope images, see figures below. A comparison of the surface of the catalyst pellets before and after use shows some possible loss in surface area although further investigation is required to substantiate this finding. The images below show the surface of a virgin and used catalyst pellet.

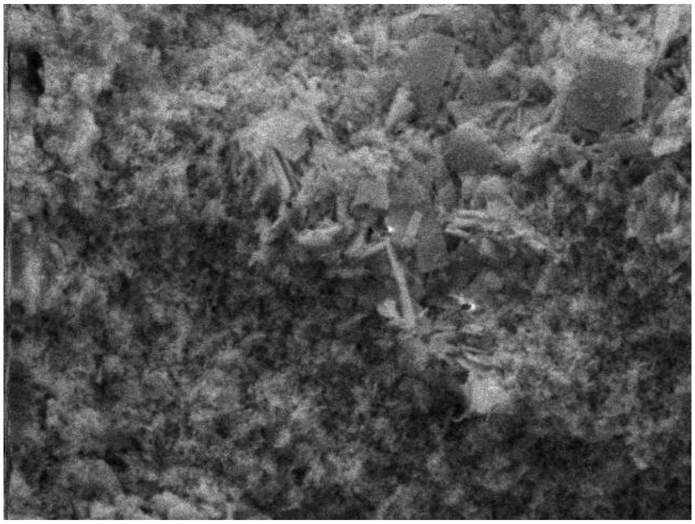

Figure 69: Virgin Catalyst surface

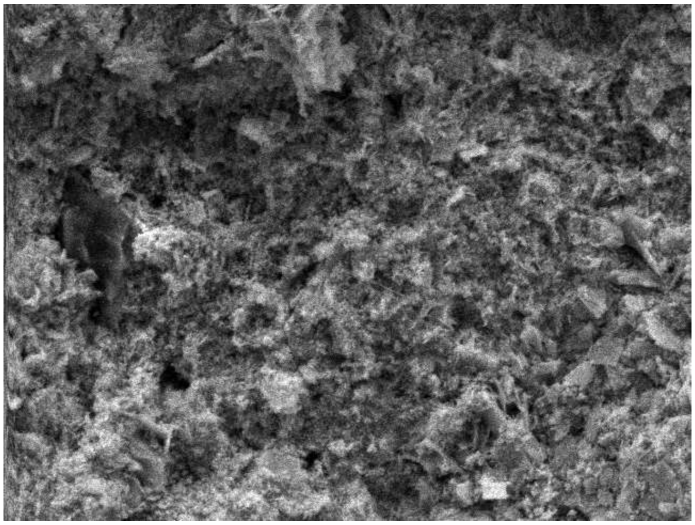

Figure 70: Virgin Catalyst surface

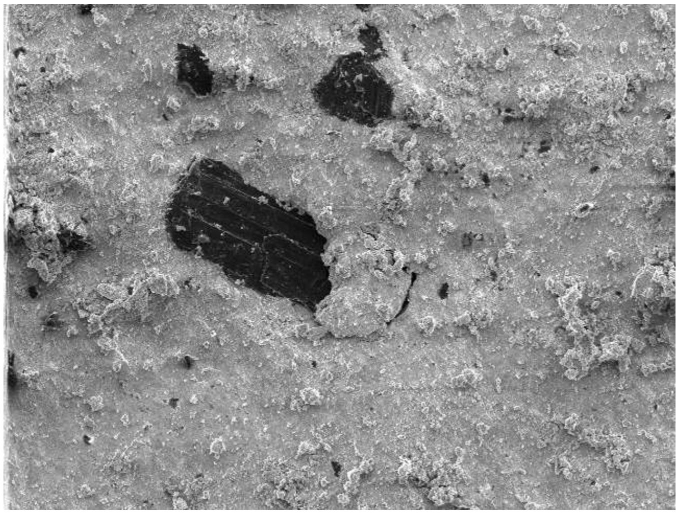

Figure 71: Virgin Catalyst surface

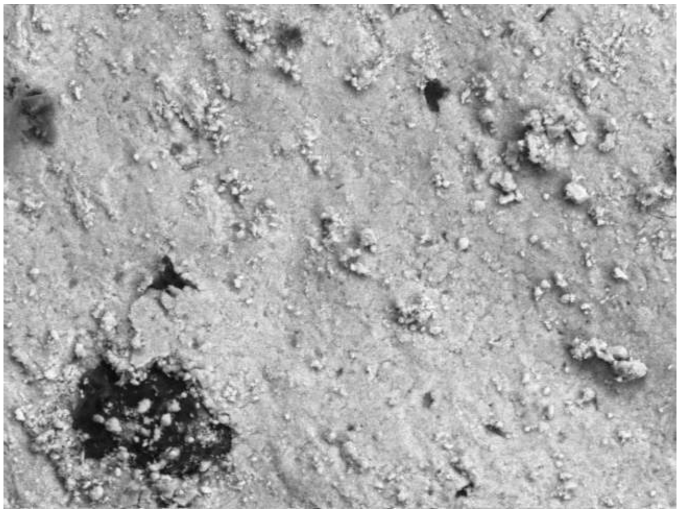

Figure 72: Used Catalyst surface

EDS results show that the bright white areas in the light microscope pictures and the dark spots in the SEM pictures are graphite islands. The copper and zinc oxides are very evenly distributed across the surface and throughout the interior of the pellets with no identifiable regions rich in either on or the other. This even distribution continues down to minimum spot size of this technique in the micrometer size scale. The figures below show the spectroscopic signatures for Copper, Zinc, Carbon and Oxygen. The distributions for the virgin and used samples tested so far show no identifiable differences.

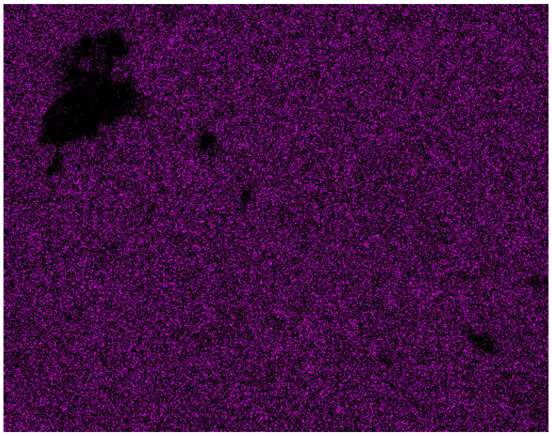

Figure 73: Virgin Catalyst surface, Copper K-alpha wavelength

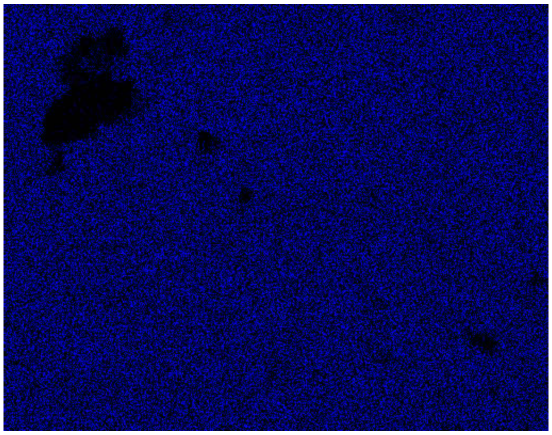

Figure 74: Virgin Catalyst surface, Zinc K-alpha wavelength

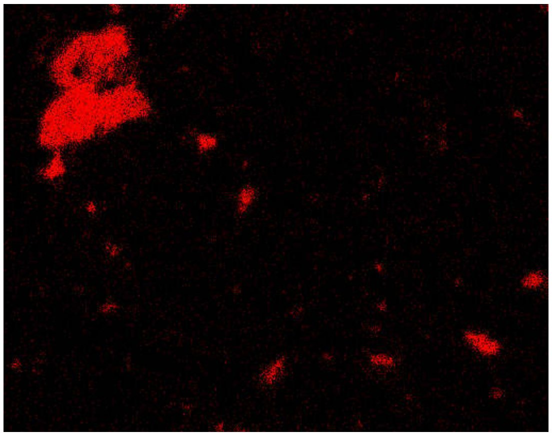

Figure 75: Virgin Catalyst surface, Carbon K-alpha wavelength

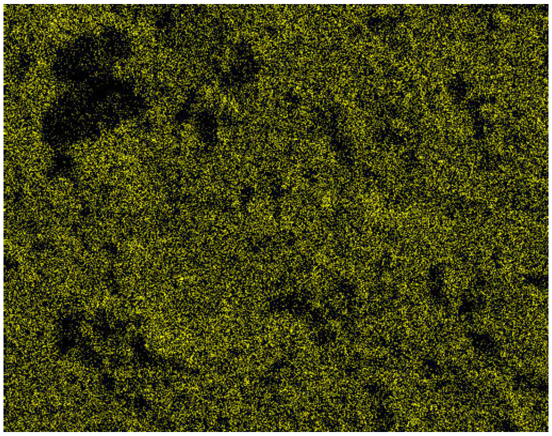

Figure 76: Virgin Catalyst surface, Oxygen K-alpha wavelength

XRD analysis has shown some differences between the virgin and used samples. The chart below shows the x-ray diffraction signature for the virgin, blue line, and used, gray line. The heights of several peaks have changed slightly showing that the crystal structure of the sample has changed slightly. To date analysis of this data has been inconclusive due to the overlap of the copper oxide and zinc oxide peaks making a peak broadening analysis to determine crystallite size impossible. The changes in oxidation state encountered in the re-oxidation process may be the cause of the differences between the virgin and used catalyst XRD signature. Further work will focus on developing the infrastructure to analyze the catalyst in reduced form in order to make stronger comparisons.

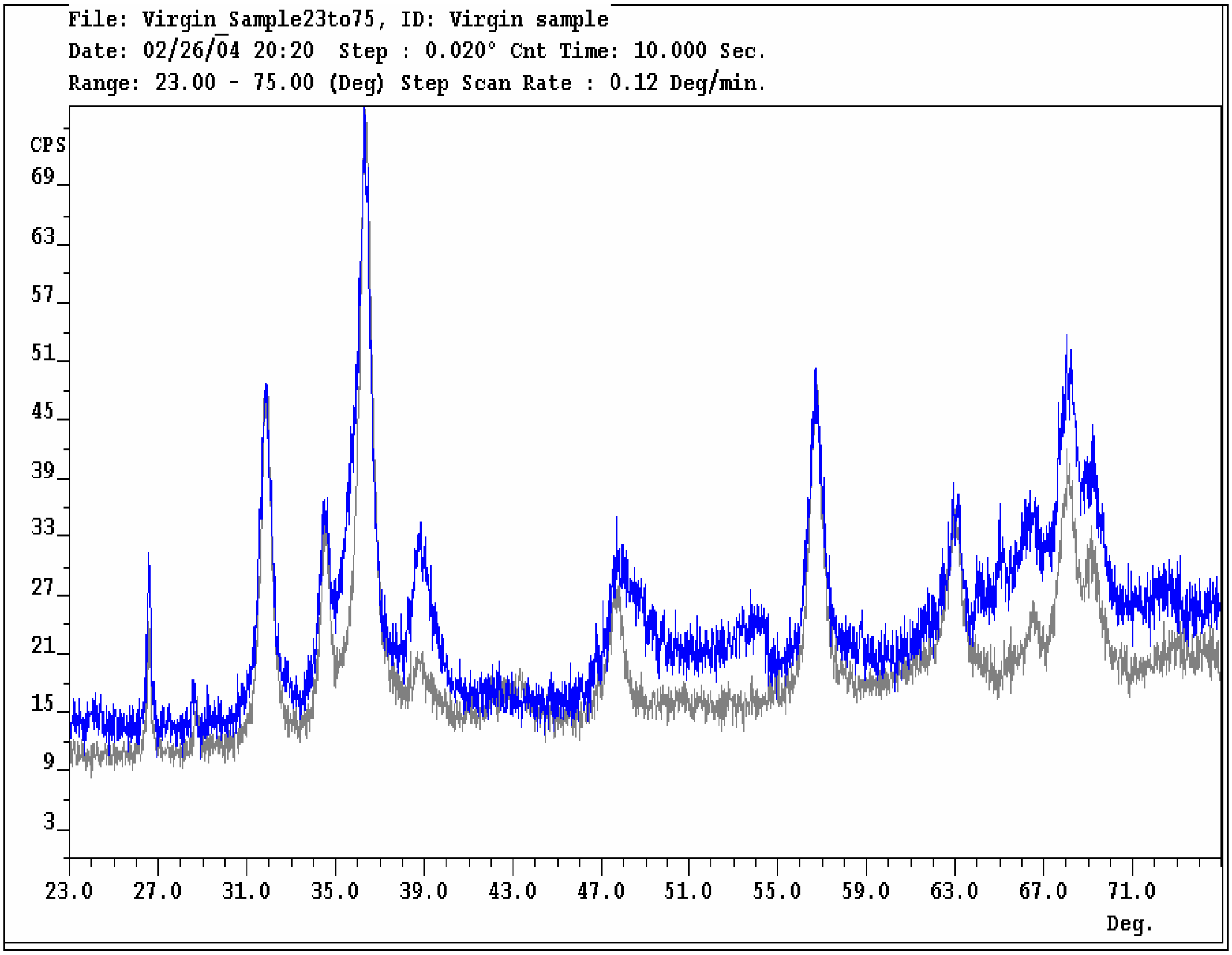

Figure 77: XRD signature for the virgin, blue line, and used, gray line, catalyst samples

Temperature Profiles

The measurement of temperature profiles in the operating reactor inform further development of reactor designs and contribute to the understanding of catalyst degradation. We are actively developing our techniques and infrastructure of measuring temperature profiles quickly and accurately. Current work is comparing temperature profiles between reactors of different aspect ration in order to find an optimum reactor geometry for maximum conversion, throughput and catalyst life.

Steam Reformation Enhancement Methods

Data of fuel-cell grade methanol with bluff bodies in Reactor B was already collected by using crushed and palletized FCRM-2 catalyst. Data of Coal-based methanol was also collected with bluff bodies in Reactor B. In crushed catalyst run, the reforming conversion shows a 5% increase for all the four different premix flow rates (5ml/min, 10ml/min, 15ml/min and 20 ml/min) compare to one without bluff body in Reactor B. The conversion vs. lhsv-m (liquid hourly space velocity of methanol) is shown in Figure 78.

Space velocity is a quasi non-dimensional term defined as volumetric flow rate through a reactor divided by the volume of the reactor (based on catalyst packing length). Liquid hourly space velocity is defined in Equation 3

$$LHSV - M = \left(\frac{\frac{m^3}{hr}\ liquid\ \ methanol\ \ input}{m^3\ reactor\ volume} \right)$$

Equation 3

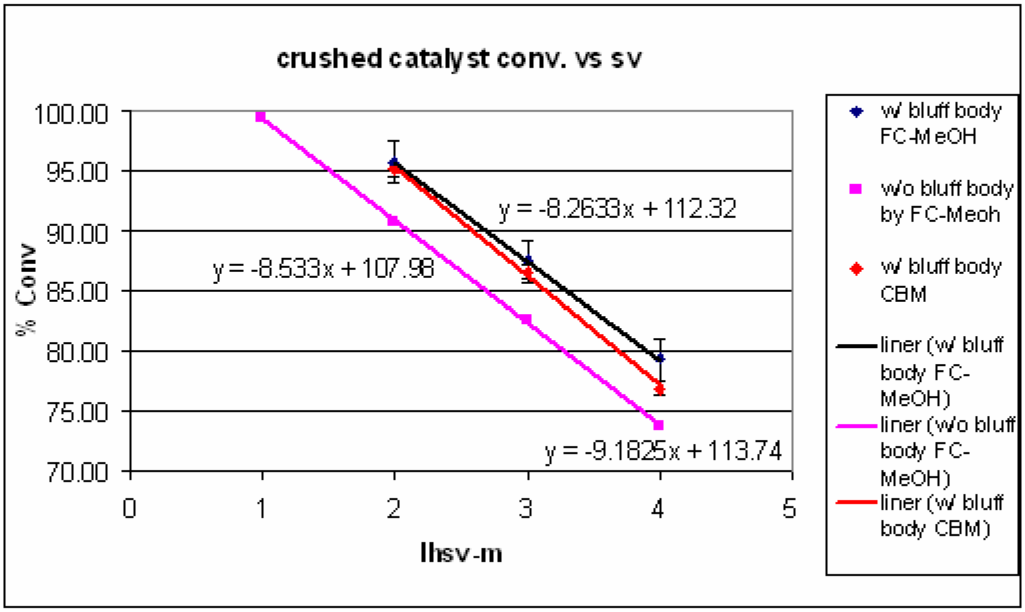

Figure 78: Conversion vs. Liquid hourly space velocity of methanol for crushed catalyst

From the data of pelletized catalyst run, the reforming conversion shows an increase tendency up to 5% as increasing the flow rate to 20 ml/min, as shown in Figure 79.

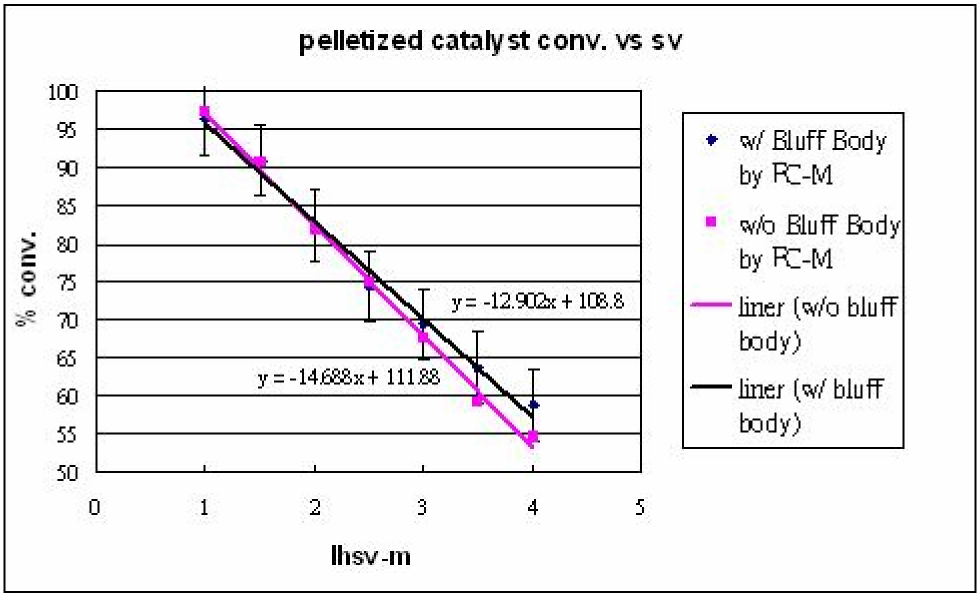

Figure 79: Conversion vs. Liquid hourly space velocity of methanol for pelletized catalyst

CONCLUSION

Much progress has been made on the project funded by the Department of Energy during this reporting period. Substantial progress on the evaluation of the composition of coal-derived methanol and the baseline fuel cell grade methanol has been made. Autothermal reactor design and construction has been initiated and continues with several integral pieces of equipment purchased and/or manufactured. Projects which have proven that coal derived hydrogen can be produced through steam reformation have been successful. Enhancement of heat transfer by bluff bodies has been proven for fuel cell grade methanol. Catalyst degradation projects have been started and analysis of reactor performance as well as catalyst analysis has taken place. Several projects are scheduled for the next quarter including validation of external evaluations of sulfur and chloride concentrations, further ATR reactor design and construction, continued preliminary evaluation of coal-based methanol in the steam reformers, and validation of heat transfer enhancement methods by use of bluff bodies.

REFERENCES

[1] The U.S Department of Energy and Air Products Liquid Phase Conversion Company, L.P Commercial-Scale Demonstration of the Liquid Phase Methanol (LPMEOH^{TM}) Process, Clean Coal Technology

[2] Erickson, P.A., Enhancing the Steam-Reforming Process with Acoustics: An Investigation for Fuel Cell Vehicle Applications, doctoral dissertation, University of Florida, Gainesville, FL, 2002

[3] J. Patrick Sterchi, The effect of Hydrocarbon Impurities on the Methanol Steam Reforming Process for Fuel Cell Applications, doctoral dissertation, University of Florida, Gainesville, FL, 2001

[4] Pio Fornzzati, Luca Lietti, Catalyst deactivation, Catalysis today 52(1999) 165-181

[5] Calvin. H. Bartholomew, Mechanism of Catalyst deactivation, Applied Catalysis A: General 212 (2001) 17-60.

[6] C.J. Jiang, D.L. Trimm and M.S. Wainwright, Kinetic mechanism for the reaction between methanol and water over a $Cu-ZnO-Al_2O_3$ Catalyst, Applied Catalysis A: General, 97 (1993) 145-158

[7] Martyn V. Twigg and Michael S. Spencer, Deactivation of copper metal catalysts for methanol decomposition, methanol steam reforming and methanol synthesis, Topics in Catalysis Vol.22 .Nos. 3-4 April 2003.